Nansen Environmental and Remote Sensing Center

A non-profit
Research institute affiliated
With the University of
Bergen

Thormøhlensgate 47
N-5006 Bergen,
Norway
http://www.nersc.no

NERSC Technical Report no. 274

Sea ice drift analysis in the Barents Sea 2006

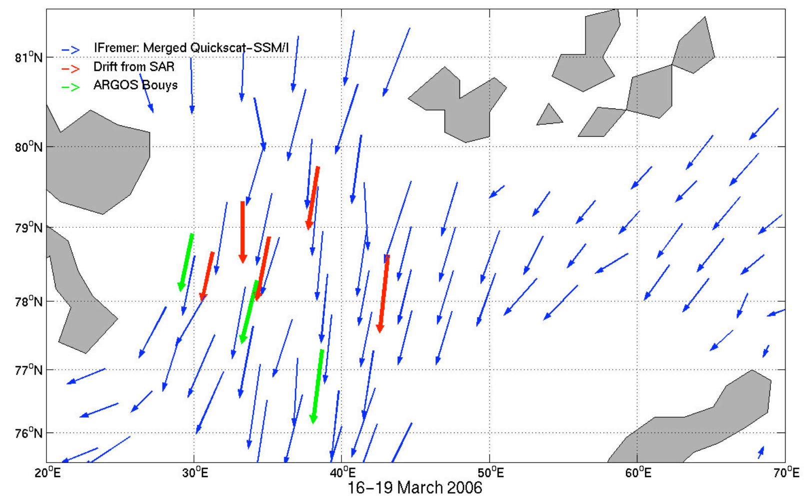

Data on sea ice drift in northeastern Barents SEa from three different sources.

Project for Statoil ASA 2006

Statoil Order no. 4501125216

Authors:
Stein Sandven, Johan Wåhlin, Morten Stette and Kjell Kloster

December 2006

Nansen Environmental and Remote Sensing Center (NERSC)

Thormøhlensgate 47
N-5006 Bergen, Norway
Phone: + 47 55 20 58 00
Fax: + 47 55 20 58 01
E-Mail: Stein.Sandven@nersc.no
http://www.nersc.no

TITLE: **Sea ice drift analysis in the Barents Seas**	**REPORT IDENTIFICATION** **NERSC Technical report no. 274**
CLIENT STATOIL ASA	**CONTRACT** Order no. 4501125216
CLIENT REFERENCE Einar Nygaard	**AVAILABILITY** Customer report
INVESTIGATORS Stein Sandven, Johan Wåhlin, Morten Stette and Kjell Kloster	**AUTHORISATION** Bergen, 22 December 2006 Stein Sandven

Contents

Executive Summary

The objective of this study was to observe sea ice drift in the Barents Sea from satellite data and in situ data from drifting ice buoys, and furthermore to use these data to validate ice drift estimates from model simulations. The background for this is the need to obtain better data on sea ice drift and iceberg drift, as well as to validate an iceberg drift model under development at NERSC. The Barents Sea had a record minimum ice extent in the spring of 2006, allowing us to study ice drift only in the northeastern part, between Novaya Zemlya, Franz Josef Land and Svalbard. Also the air temperature in this period was record high, with anomalies of 4 – 6 degrees above average. Wideswath SAR images from ENVISAT were collected from early March to late April, covering the sea ice areas roughly every three days with some interruptions. Also ASAR Global Mode data with 1 km resolution were used to estimate ice drift. The SAR ice drift vectors were compared with large scale ice drift provided by Ifremer, based on scatterometer and passive microwave data for 17 time intervals, each of three day duration. The Ifremer ice drift products are uniformly distributed in time and space, while the SAR data provides more scattered distribution of the vectors. This is due to fact that the SAR wideswath data did not cover the whole study area regularly every three days. The SAR ice drift and Ifremer ice drift showed very good agreement, and the SAR data with higher resolution could therefore be used to validate the Ifremer products. Three drifting ice buoys from CMR were deployed on ice floes and produced in situ ice drift continuously until the buoys drifted into open water southeast of Svalbard. During a three day period from 15 to 18 March, simultaneous ice drift data were obtained from both SAR and the drifting buoys. The two ice drift data sets were consistent, showing that the SAR retrieval was very close to the buoy data for the three mean drift: the displacement from SAR was 63.0 km and from the buoys 64.4 km. The direction of the drift was 190° from SAR and 196° from the buoys. The TOPAZ model simulations of ice drift were compared with the observed ice drift from SAR and Ifremer for the 17 time intervals. There was generally good agreement between the observed and modeled ice drift. The present study has used a three day interval for the ice drift, but it is necessary to compare ice daily averaged ice drift, because we know that ice drift can change rapidly in this region due to changing wind forcing. It is important to assess how well satellite data can be used for monitoring daily ice drift. Data on sea ice drift will be an important component of the validation of the Barents Sea model that includes an iceberg drift model. It is recommended to continue observation of sea ice properties as part of the iceberg modelling work in the Barents Sea. The goal for this work is to come up with a monitoring and forecasting system for sea ice and icebergs, using numerical models in combination with satellite data and drifting ice buoys.

1. Overview of the ice season 2006 and comparison with previous years

The sea ice in the Barents Sea during winter and spring 2006 was charaterized by minimum extent, where only the northeastern part was ice covered in April, the month of maximum ice extent. The seasonal and interannual variability of the ice extent in the Barents Sea have been monitored regularly with passive microwave satellite data for more that 25 years, and time series of 3-monthly mean ice area for the Barents Sea is shown in Fig. 1. The blue line shows that 2005 had the lowest ice area since the start of the time series in 1979. Data for 2006 are not yet included in Figure 1, but comparison between daily ice maps (Fig.2) shows that the winter of 2006 had even less ice than 2005.

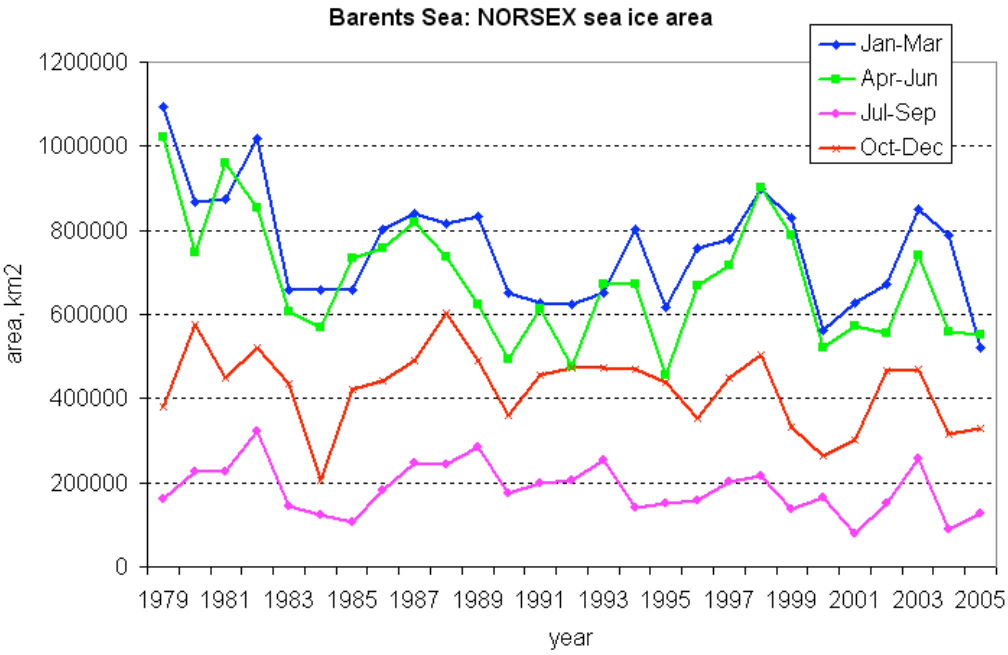

Figure 1. Time series of ice area in the Barents Sea from passive microwave satellite data (SSMI) from 1979 to 2005, presented as 3-monthly mean ice area.

The eastern Barents Sea, including Pechora Sea and the coastal region west of Novaya Zemlya, are normally ice covered in the winter months, but in 2006 there was only scattered, thin ice in this region in March and April. This is similar to the situation in the winter of 2005 when record low ice extent was observed in the passive microwave data (Fig. 1). In early March the ice extent in the northern and eastern Barenst Sea was similar in 2005 and 2006, with open water extending northeastwards to Cape Chelania, the northern tip of Novaya Zemlya (Fig. 2 a) . During the month of March the ice extent did not change much in 2005, while it retreated northwards in 2006 as a polynya opened up west of Franz Josef Land. A month later, towards the end of April, the ice border in 2005 was located between Hopen and the coast of Novaya Zemlya at 75 N. This is the period when the ice exent is normally at a maximum in the Barents Sea. In 2006, the ice edge continued to retreat northwards during April, with the open water boundary located as far north as the strait between Svalbard and Franz Josef Land (Fig. 2 c). Large areas of open water was also observed north of Svalbard, due to predominantly southerly winds in April. The development of the ice extent in 2006 is presented in a series of ice maps from January to July with10-15 days interval (Figs. 3, 4 and 5).

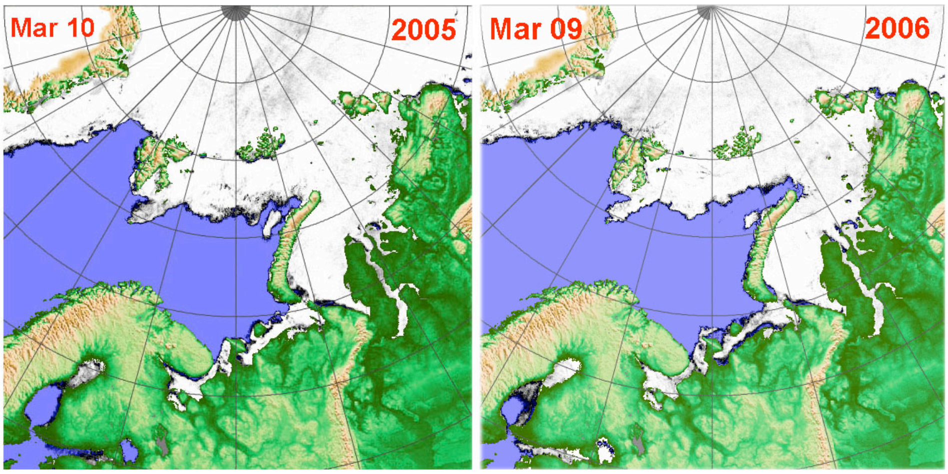

a

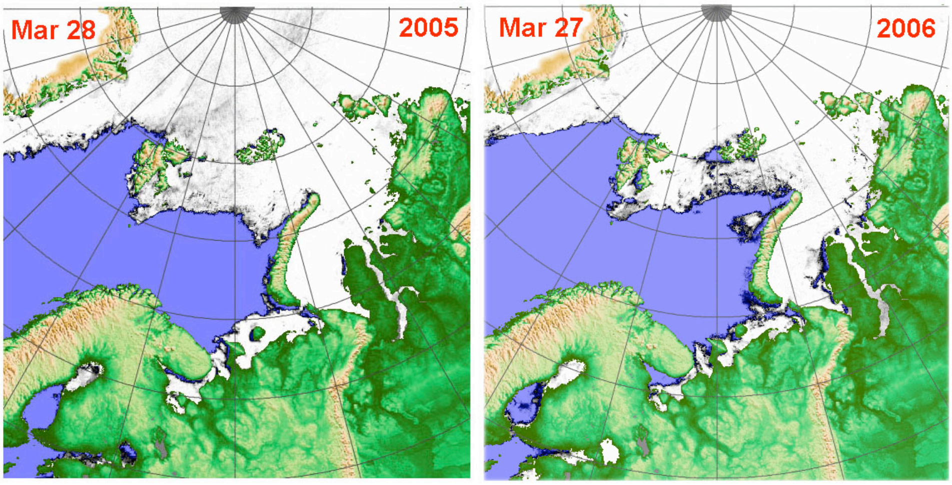

b

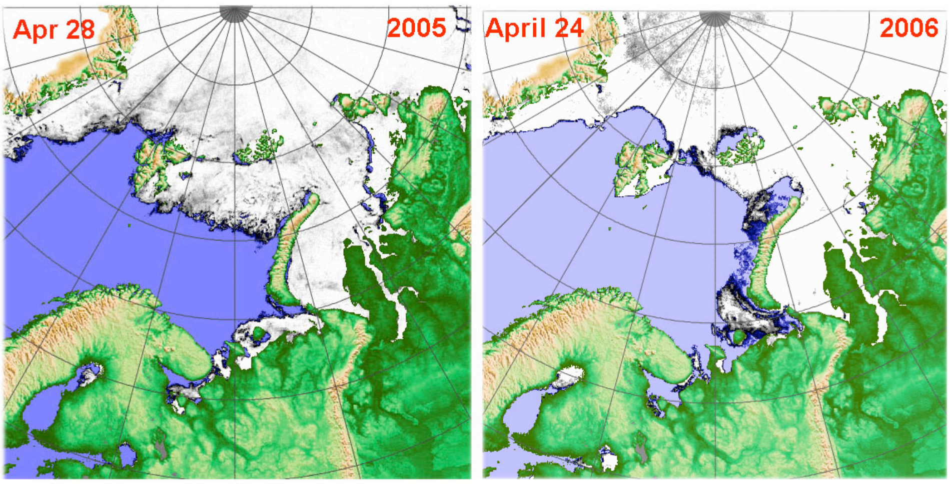

c

Figure 2. Comparison of ice area maps from AMSRE data for March and April 2005 and 2006 (Institute of Environmental Physics, University of Bremen).

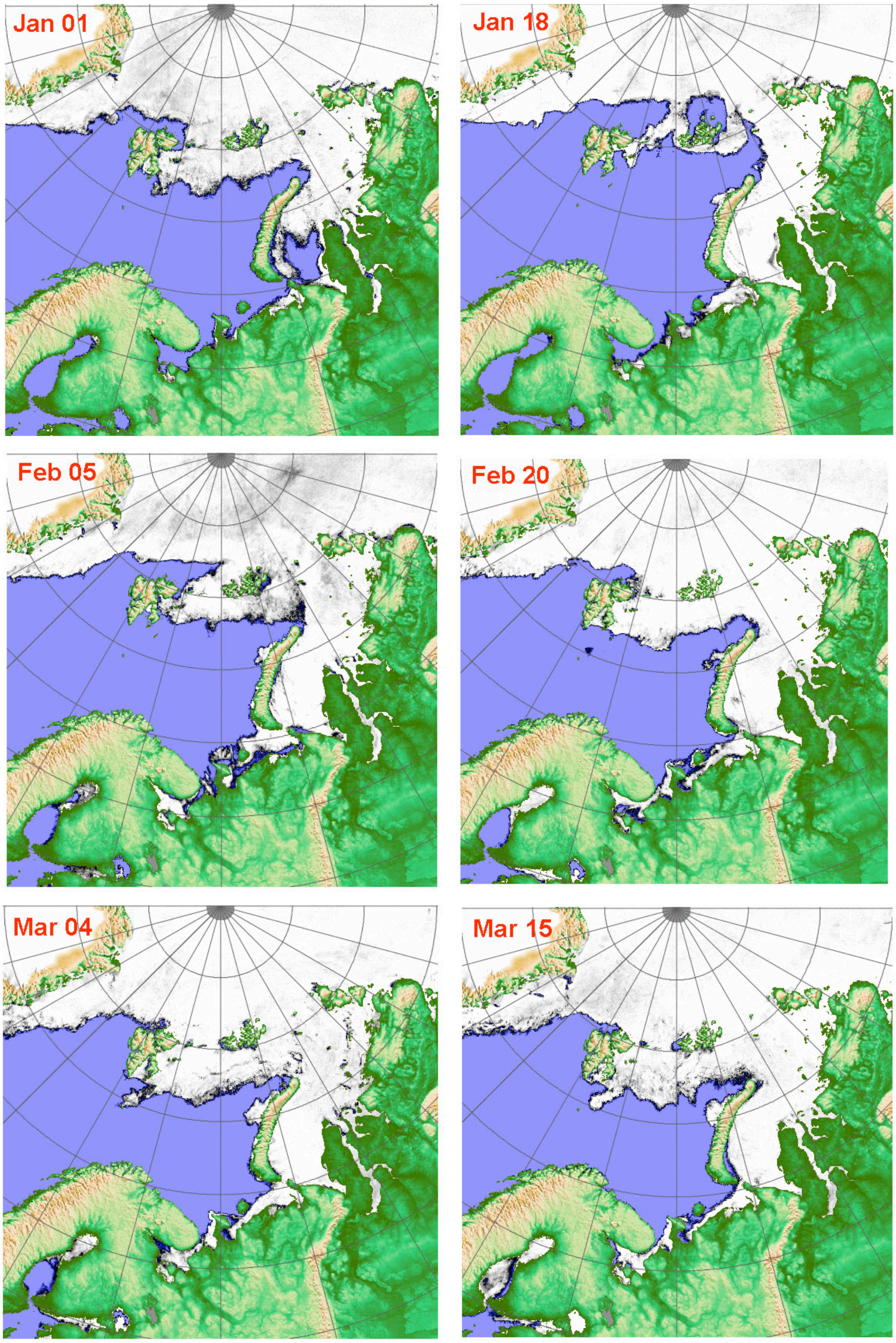

Figure 3. Ice extent maps from AMSR-E data for selected days in January – March 2006. (Institute of Environmental Physics, University of Bremen)

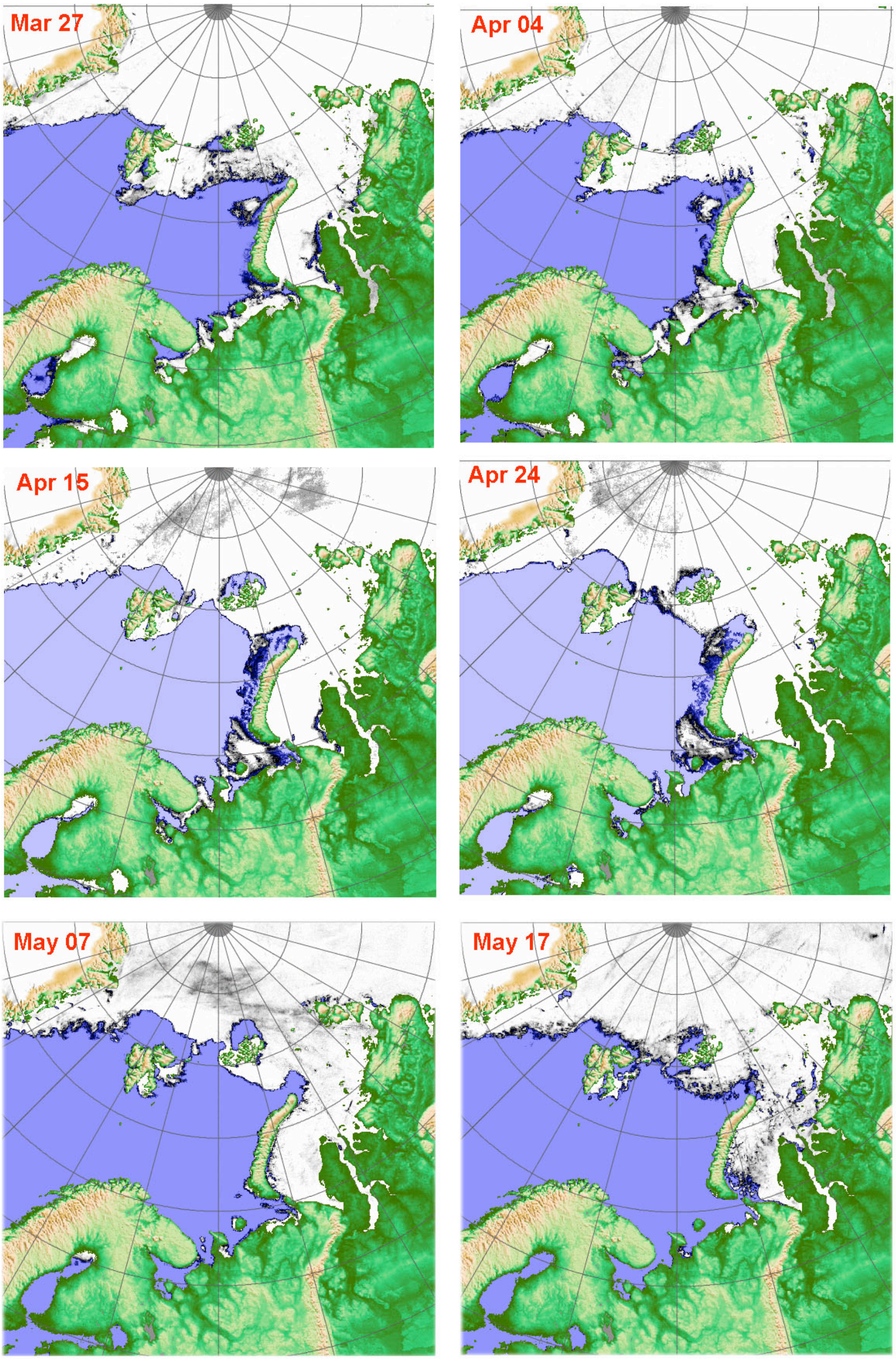

Figure 4. Ice extent maps from AMSR-E data for selected days March – May 2006. (Institute of Environmental Physics, University of Bremen)

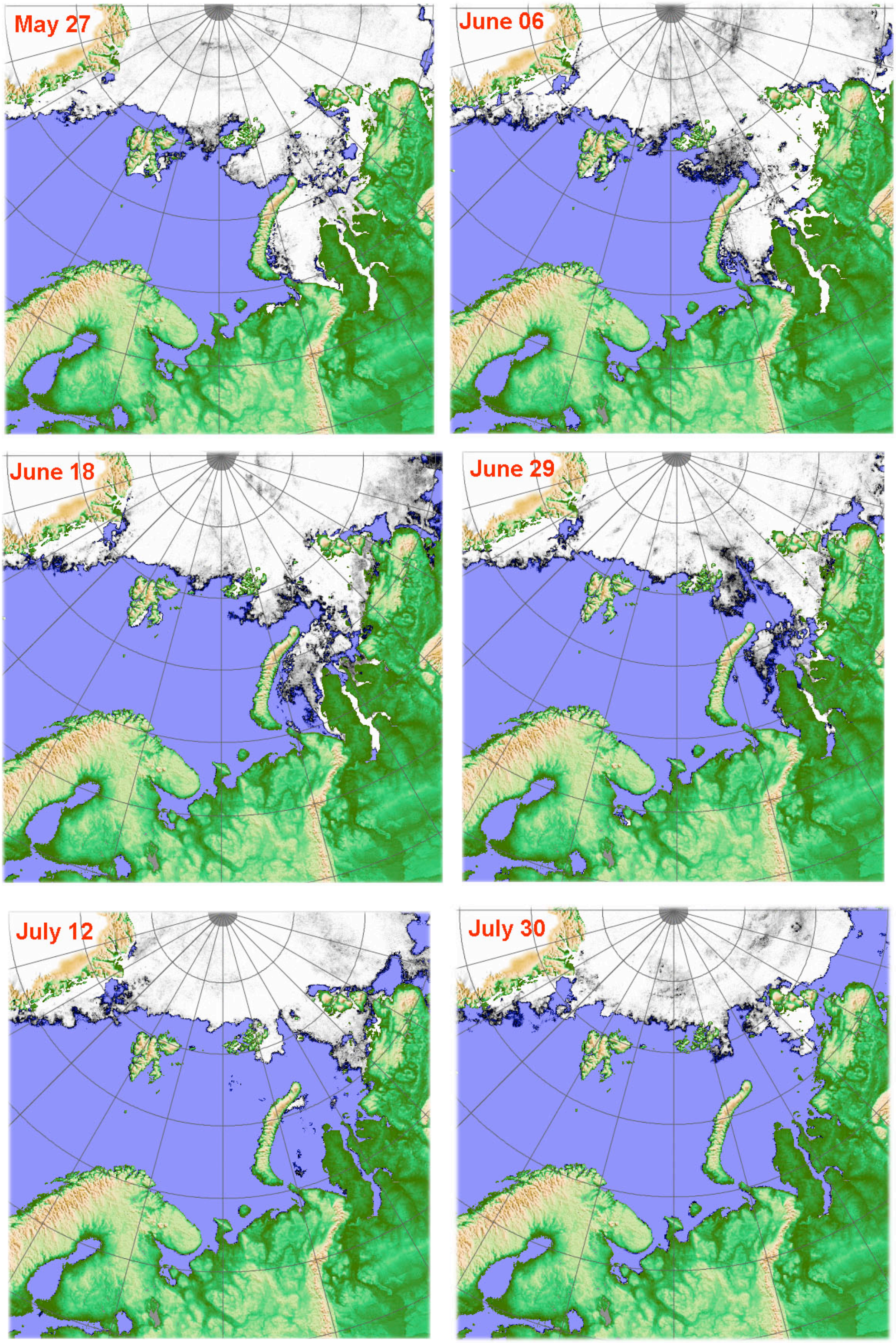

Figure 5. Ice extent maps from AMSR-E data for selected days May - July 2006. (Institute of Environmental Physics, University of Bremen)

2. Atmospheric and oceanographical conditions

Both the atmosphere and the ocean have shown significantly high temperatures in the winter of 2006 compared to previous winters. While 2005 had a mean positive temperature anomaly of 2 – 4 dec C in the high Arctic, the warming was enhancede in the first half of 2006, with maximum anomaly of 4 – 6 deg C in the northern Barents Sea (Fig. 6). Ocean temperature has increased significantly in the recent years. For example, the water masses in the upper 500 m in the Fram Strait have become warmer and saltier (the Atlantic inflow) as shown in Fig. 7.

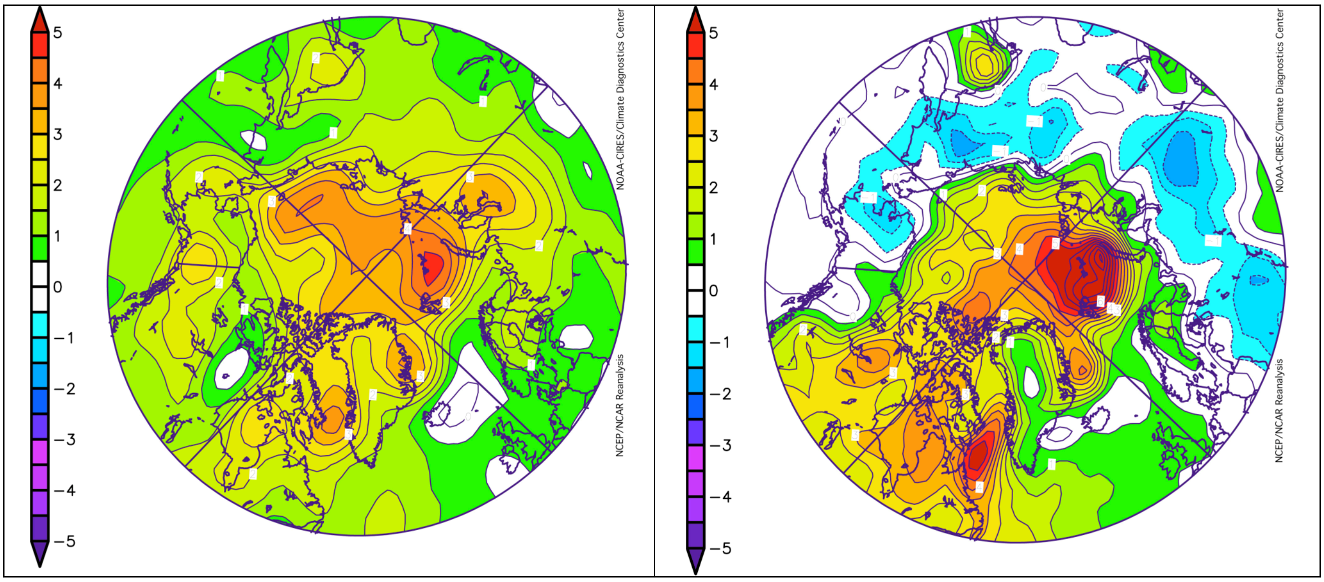

Figure 6. Surface air temperature anomalies in the Arctic and sub-Arctic regions from NCEP/NCAR reanalysis: (a) mean anomaly for whole 2005, (b) mean anomaly for January to July 2006.

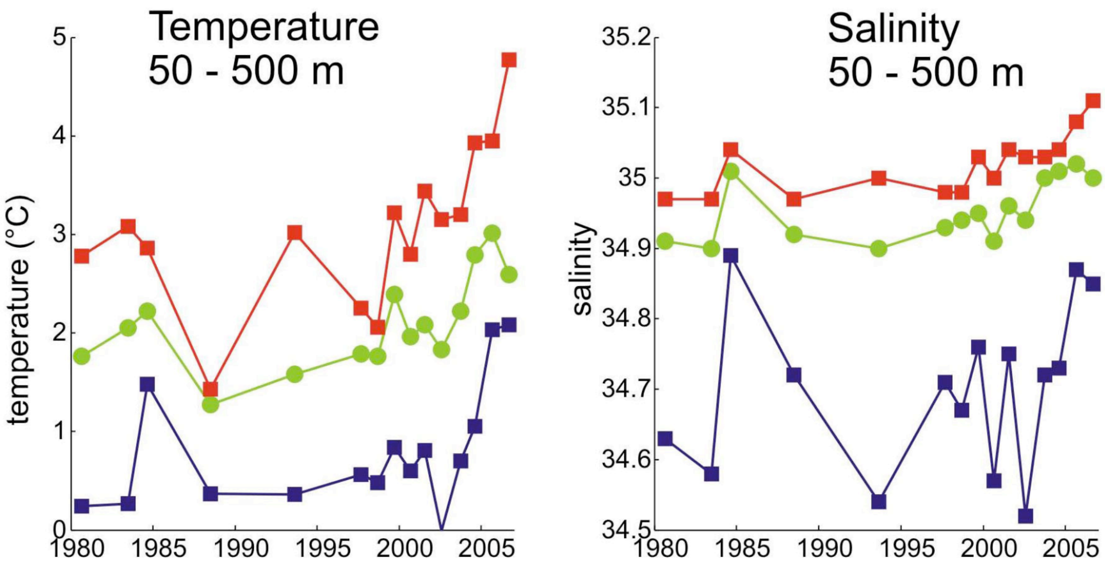

Figure 7. Changes in ocean temperature and salinity in the Fram Strait over the last 25 years based on hydrography data (from U. Schauer, AWI).

Institute of Marine Research reported record high winter temperature in the Barents Sea in March 2006 (http://www.imr.no/aktuelt/nyhetsarkiv/2006/mars). The inflow of Atlantic water to the Barents Sea was 1.5°C higher than normal in January. The previous winter temperature at this level was observed in 1938/39. After a minimum in the late 1960s, the temperature has shown an increasing trend.

3. Ice drift study in spring 2006

3.1 Deployment of drifting ice buoys

Three ice buoys delivered by CMR were deployed on ice floes in the area between Svalbard and Franz Josef land in early March. The objective of this experiment was to measure the ice drift accurately using GPS positions, and to use these data for validation of ice drift derived from satellite data and ice drift simulations from models. On this background, intensified SAR data acquisition was done in the period March – April for estimation of ice drift from SAR data. In this period the sea ice was only located in the northeastern part of the Barents Sea (Fig. 3 and 4).

3.2 SAR data acquisition

Wideswath SAR data from ENVISAT were obtained almost every day in March and April, but the data coverage varied from day to day. In order to calculate ice drift we selected SAR images with three day interval. Three days represent a subcycle of the ENVISAT orbit allowing repeated data coverage over almost the same area. In addition to the Wideswth data, we also tested the capability to use ASAR Global Mode data which are obtained regularly over the Arctic sea ice. The ASAR Global Mode data have coarser resolution (≈ 1 km) and the possibility to retrieve ice drift is possibly not as good compared to the Wideswath images. Table 1 gives an overview of the three-day intervals for which ice drift has been calculated using both Wideswth and Global Mode data from ENVISAT ASAR.

Table 1. Three-day intervals used for SAR data collection and ice drift analysis

3-day	Wide swath		Global mode		Bouy data	
intervals	Time (GMT)	No of obs	Time (GMT)	No of obs	Time	No of daily mean
2/3 – 5/3	16:24 – 16:30	21	08:08 – 08:14	4		
14/3 – 17/3	16:45 – 16:49	8	08:32 – 08:31	2		3
15/3 – 18/3	16:15 – 16:21	11	08:01 – 08:06	2		3
28/3 – 31/3	16:07 – 16:13	16				
29/3 – 1/4	15:36 – 15:41	9	07:14 – 07:19	10		
30/3 – 2/4	16:43 – 16:46	13				
31/3 – 3/4	16:13 – 16:18	17	07:59 – 08:05	10		
1/4 – 4/4	17:19 – 17:27	14	07:19 – 07:25	9		
10/4 – 13/4	17:39 – 17:42	2				
11/4 – 14/4	15:27 – 15:33	8	07:06 – 07:11	8		
12/4 – 15/4	16:36 – 16:42	11	09:54-10:00	1		
13/4 – 16/4	16:04 – 16:10	16	09:24 – 09:29	1		
14/4 – 17/4	15:33 – 15:38	9	07:11 – 07:26	5		
15/4 – 18/4	16:42 – 16:47	9				
16/4 – 19/4	16:10 – 16:16	11	07:56 – 07:54	5		
17/4 – 20/4	17:17 – 17:25	6	07:26 – 07:32	3		
25/4 – 28/4	16:27 – 16:33	8				

The table also indicates how many ice dirft vectors were retrieved from pairs of images, using manual analysis. The automatic ice drift retieval algorithm was not used in this study because we wanted to have the ice drift estimates as accurately as possible. This could best be obtained by manual analysis where ice floes, leads and other ice features are accurately geolocated and displacement of the features are determined.

In addition to ASAR data we also included ice drift data from Ifremer based on scatterometer and passive microwave satellite data. The data from the drifting buoys where included in the period 14 – 18 March when buoy data were available at the same time as the satellite-based ice drift data. The buoy trajectories between 03 March and 12 April are shown in Fig. 8. At the end of this period the buoys had drifted out in open water east of Edgeøya.

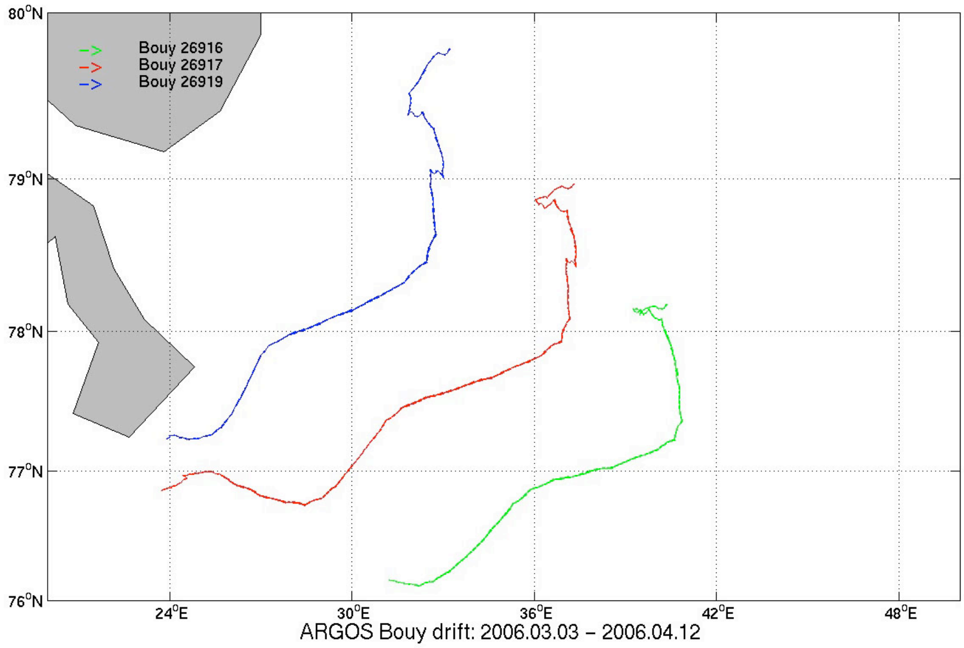

Figure 8. Trajectories of the three drifting buoys from 03 March to 12 April 2006.

3.3 Ice drift analysis

The ice drift analysis were performed with the following objectives:

(1) Study how good SAR Wideswath images are for estimation of ice drift in the Barents Sea;
(2) Compare SAR ice drift with data for the three drifting buoys
(3) Compare SAR ice drift with Ifremer's ice drift based on scatterometer and passive microwave data (Quikscat and SSMI data)
(4) Perform the first tests of ice drift retrieval from ASAR Global Mode data and comparison with other ice drift data
(5) Validation of modelled ice drift from TOPAZ, which is nested with the Barents Sea model.

The following plots show the results of the ice drift analysis from satellite data, drifting buoys and model forecasts.

Ice drift from Wideswath SAR, Quikscat/SSMI and TOPAZ modelling and assimilation system

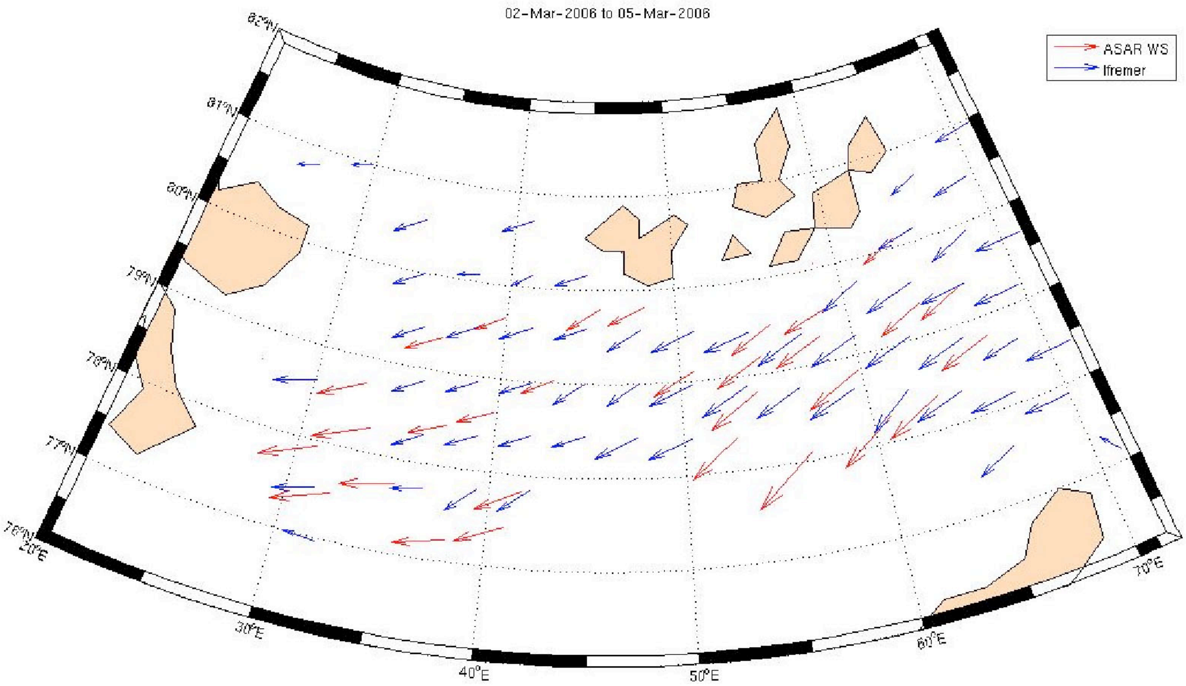

a

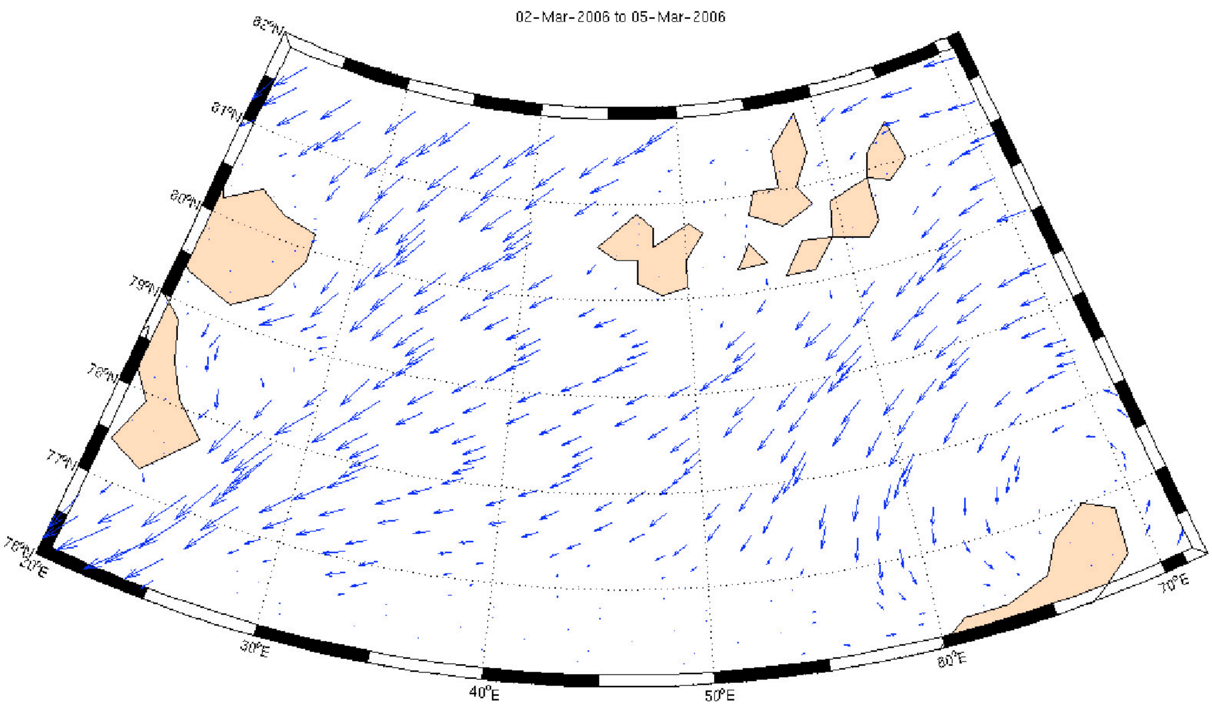

b

Figure 9. Sea ice drift from satellite data (a) and from the TOPAZ system (b) for 02-05 March 2006

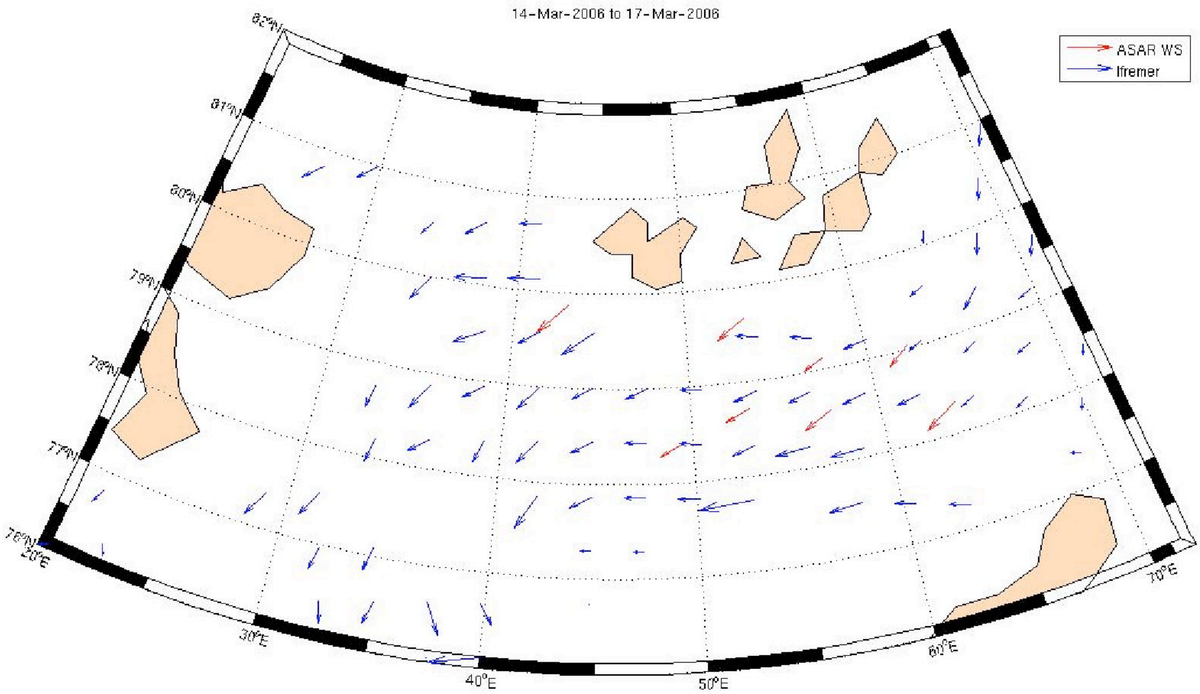

a

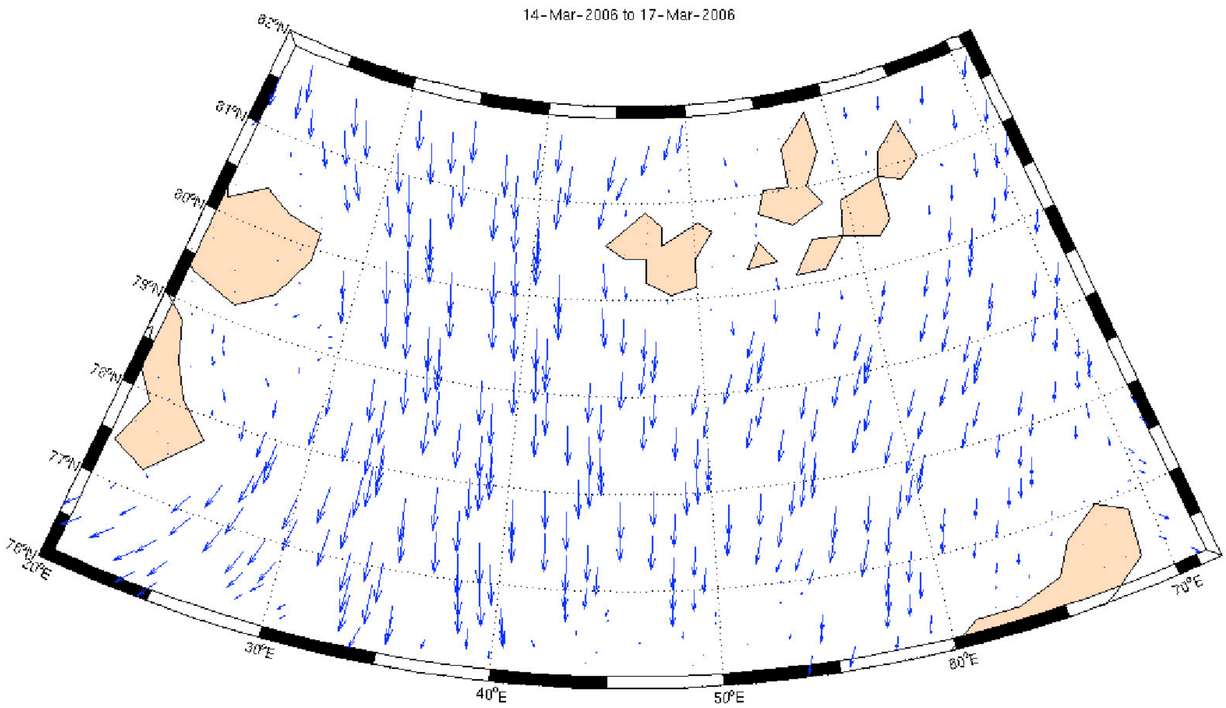

b

Figure 10. Sea ice drift from satellite data (a) and from the TOPAZ system (b) for 14-17 March 2006

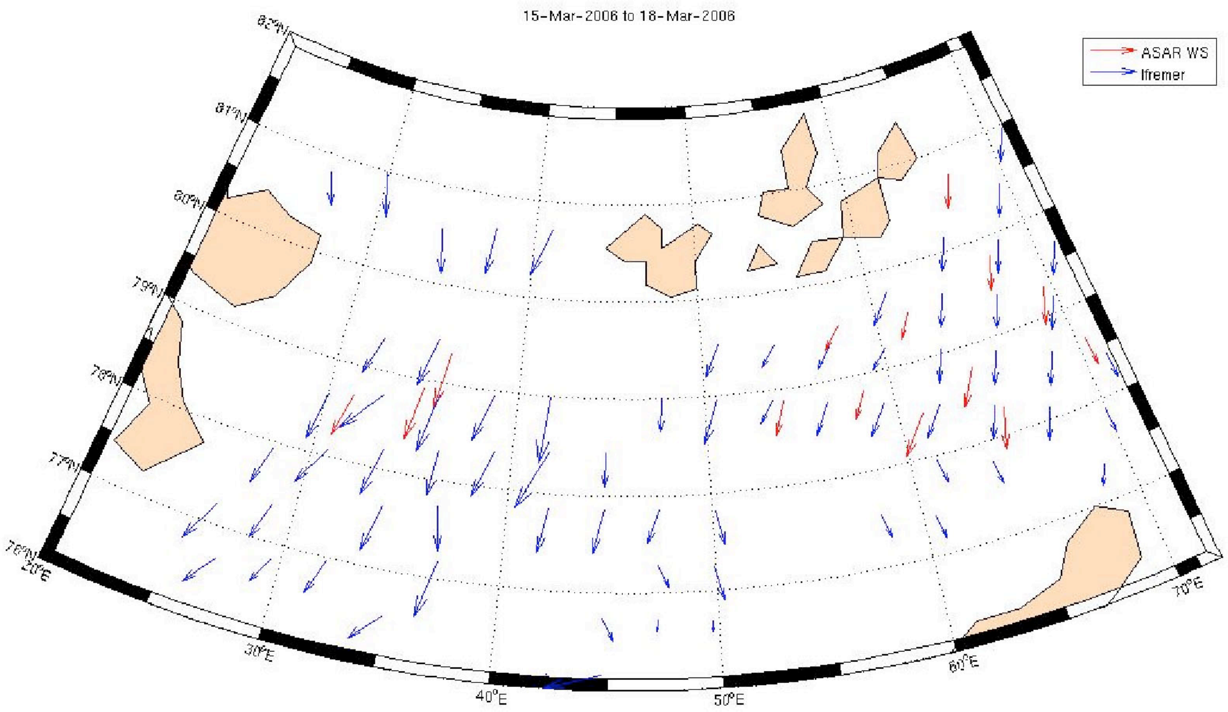

a

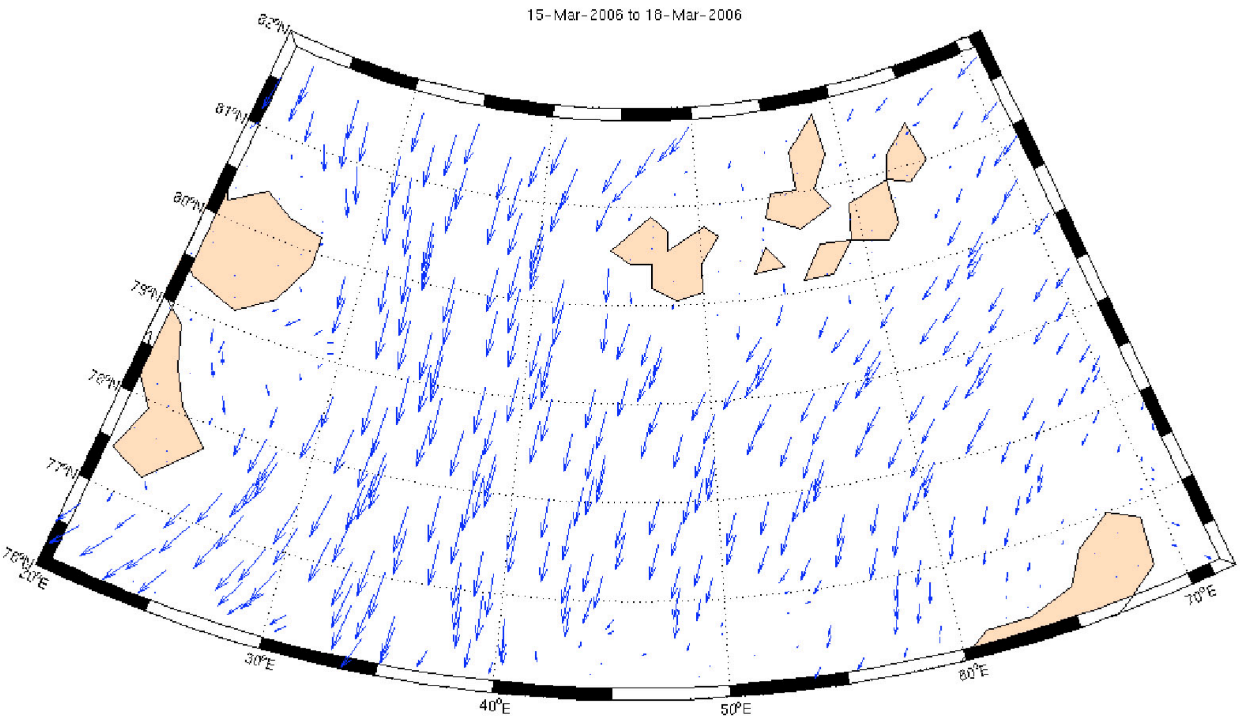

b

Figure 11. Sea ice drift from satellite data (a) and from the TOPAZ system (b) for 15-18 March 2006

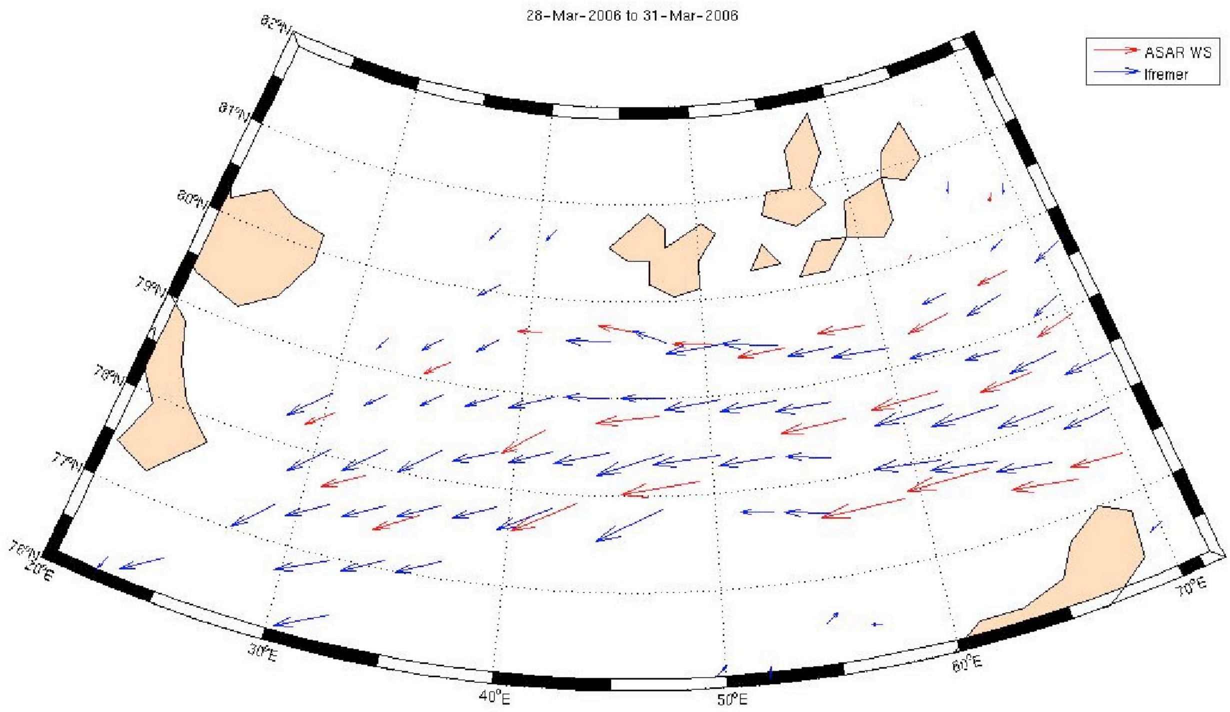

a

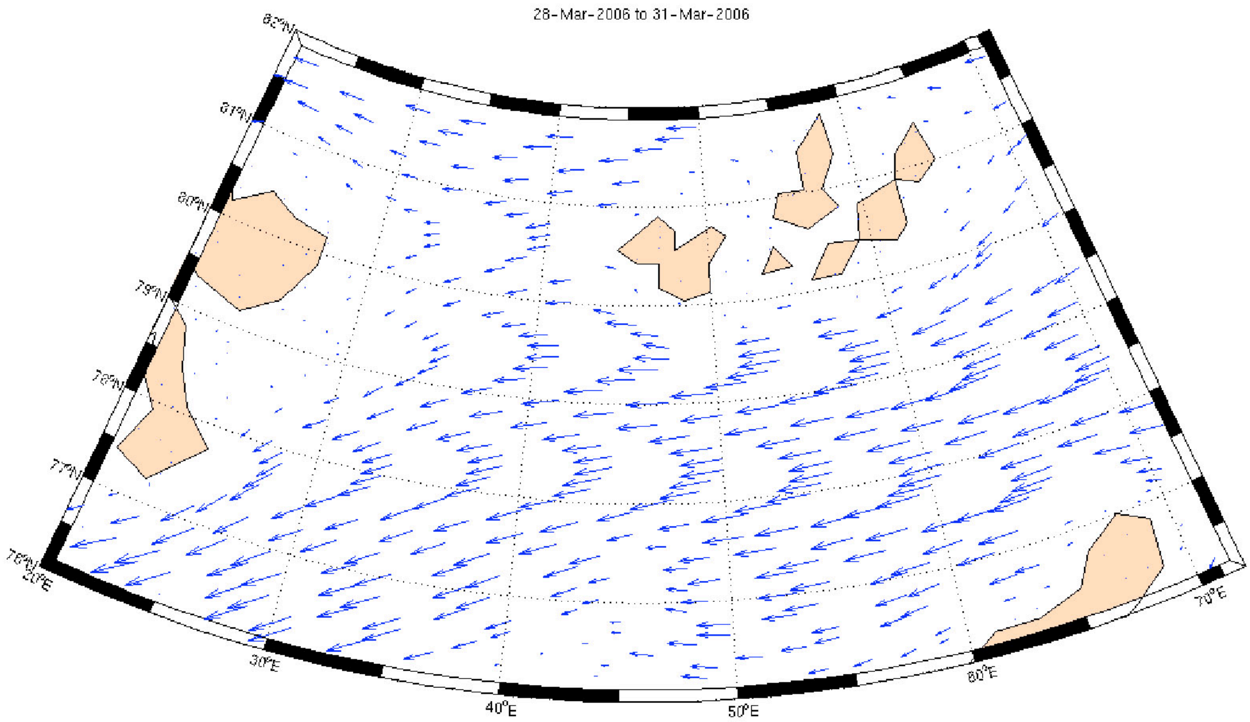

b

Figure 12. Sea ice drift from satellite data (a) and from the TOPAZ system (b) for 28-31 March 2006

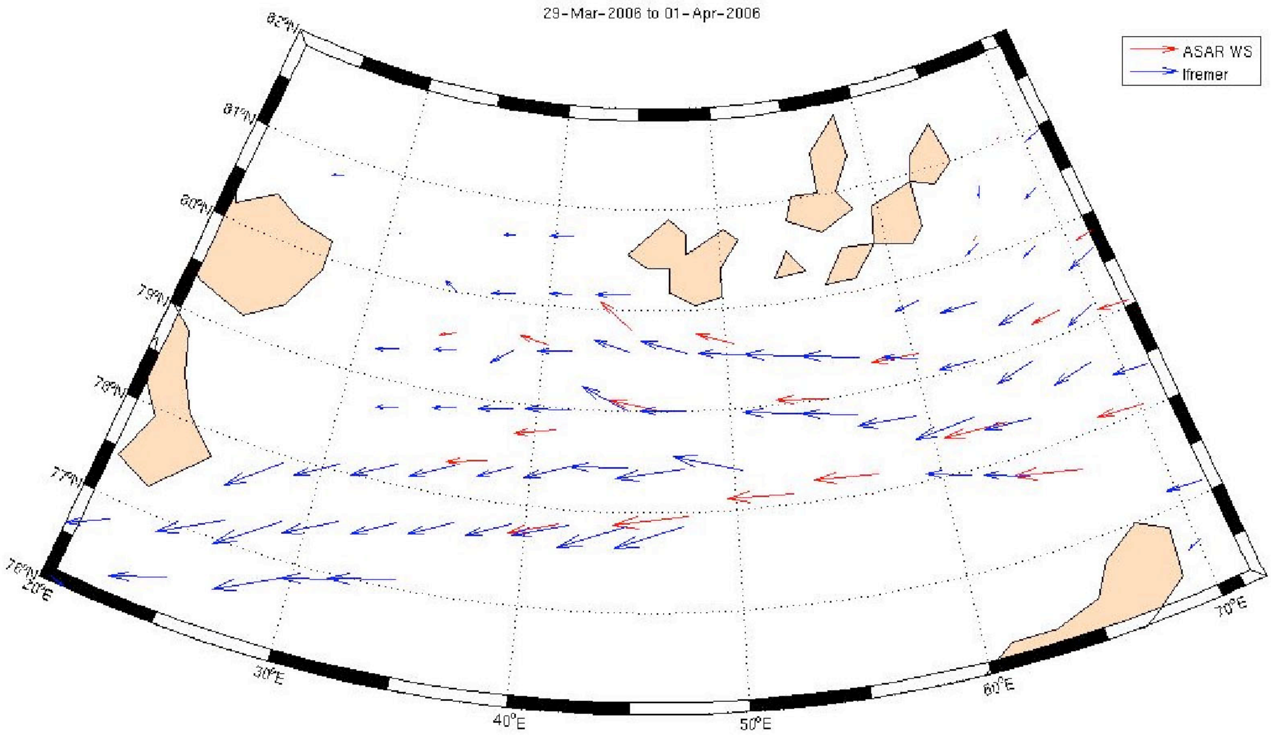

a

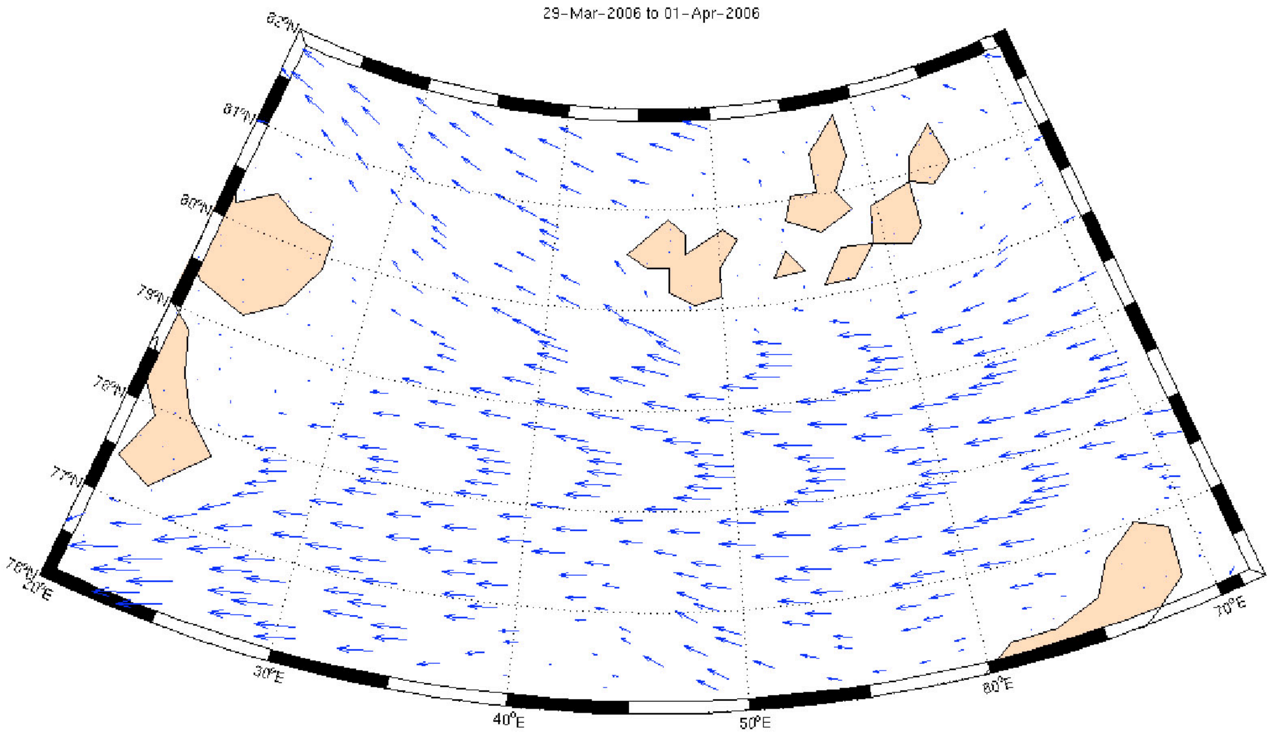

b

Figure 13. Sea ice drift from satellite data (a) and from the TOPAZ system (b) for 29 March- 01 April 2006

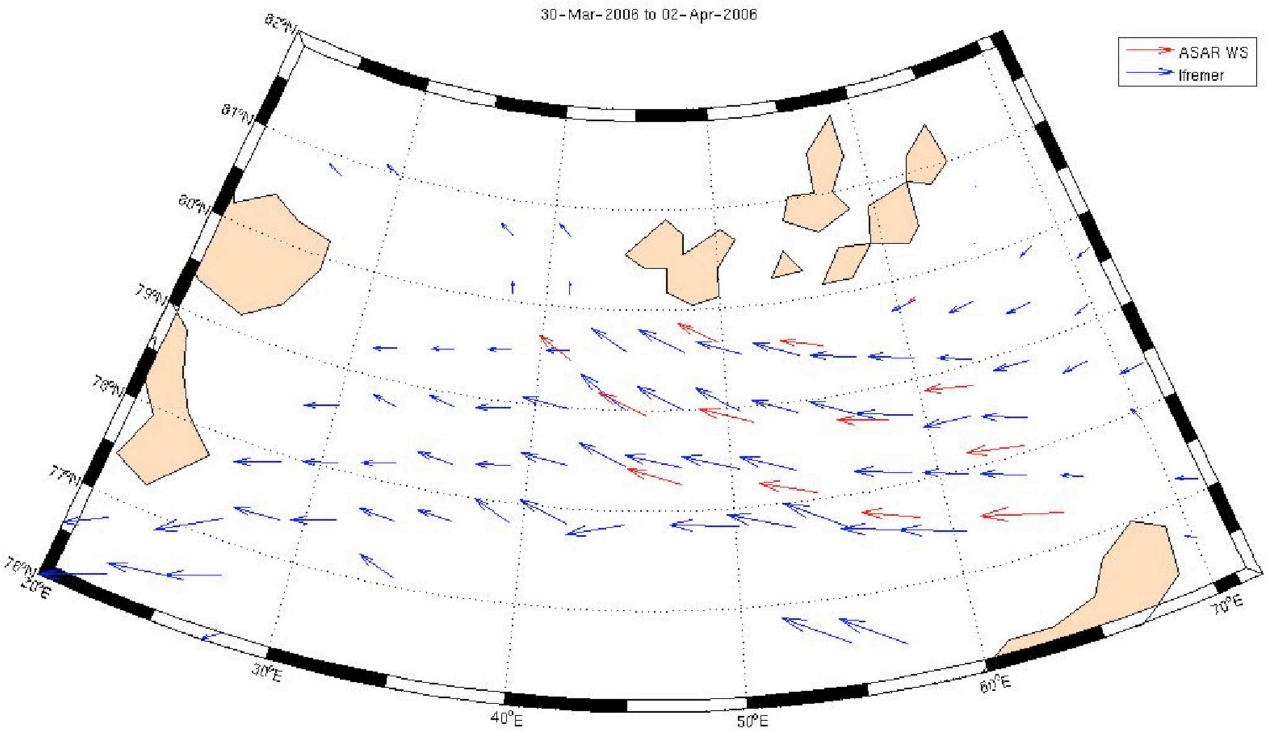

a

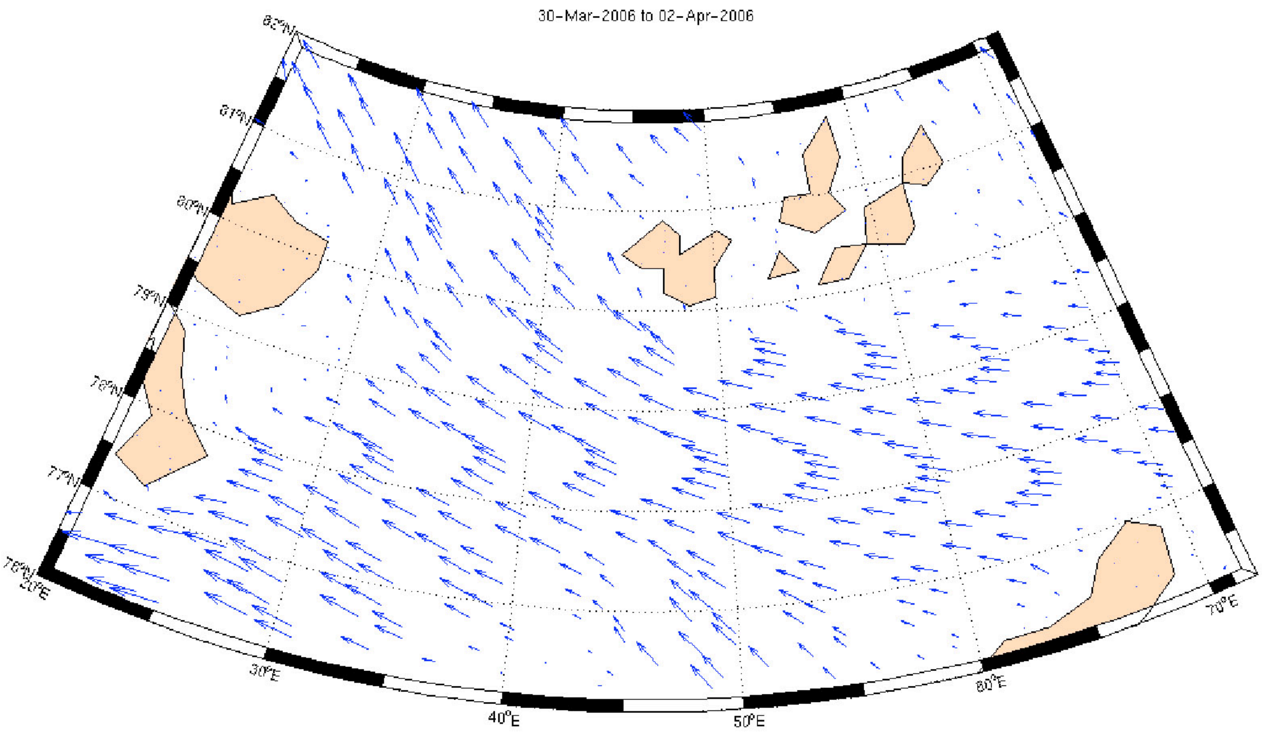

b

Figure 14. Sea ice drift from satellite data (a) and from the TOPAZ system (b) for 30 March – 02 April 2006

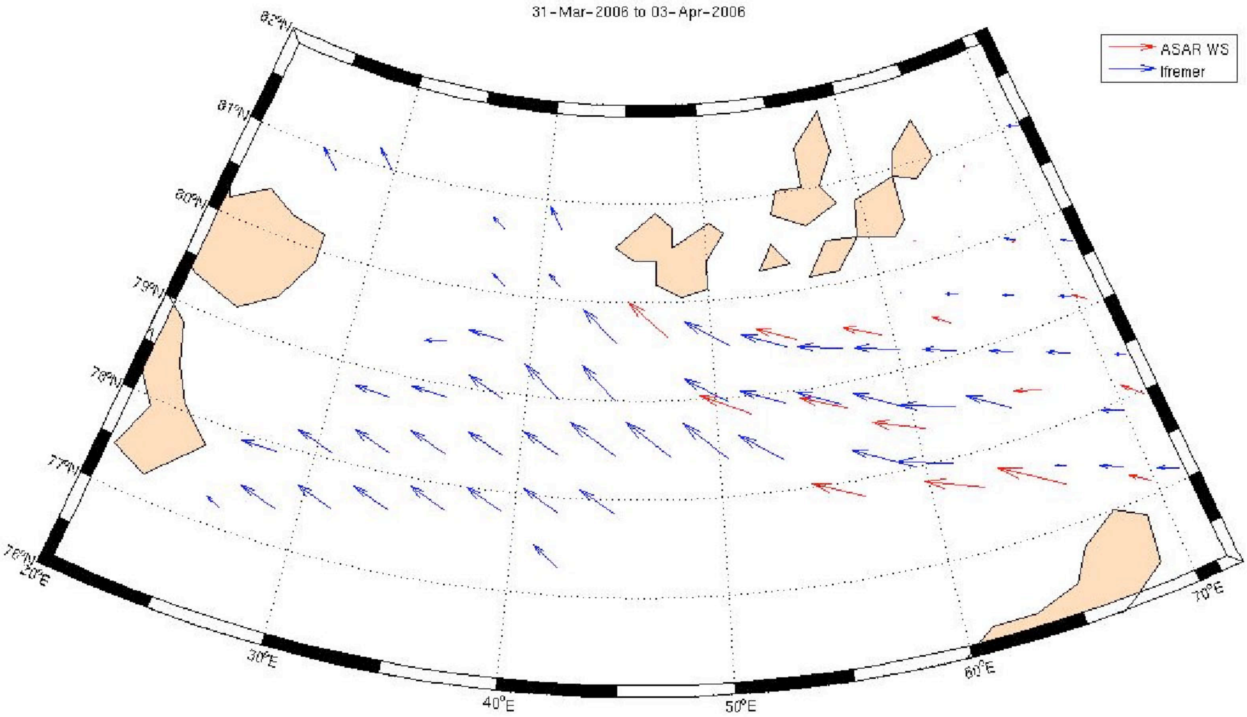

a

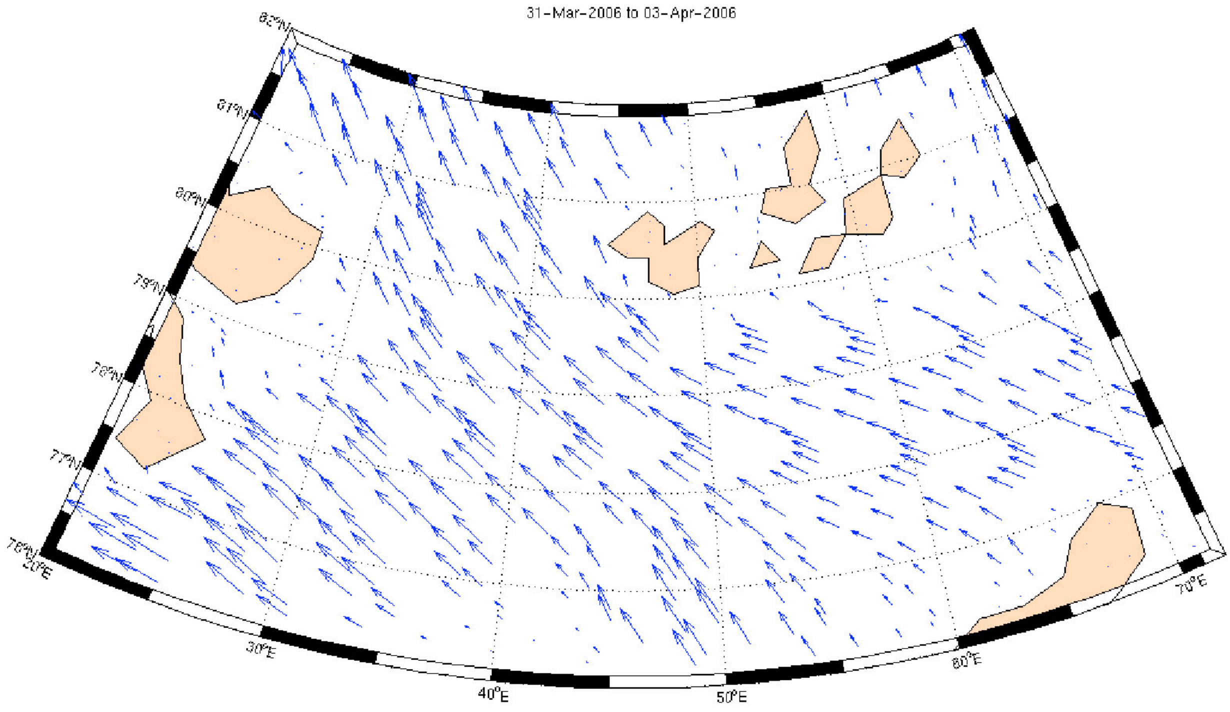

b

Figure 15. Sea ice drift from satellite data (a) and from the TOPAZ system (b) for 31 March – 03 April 2006

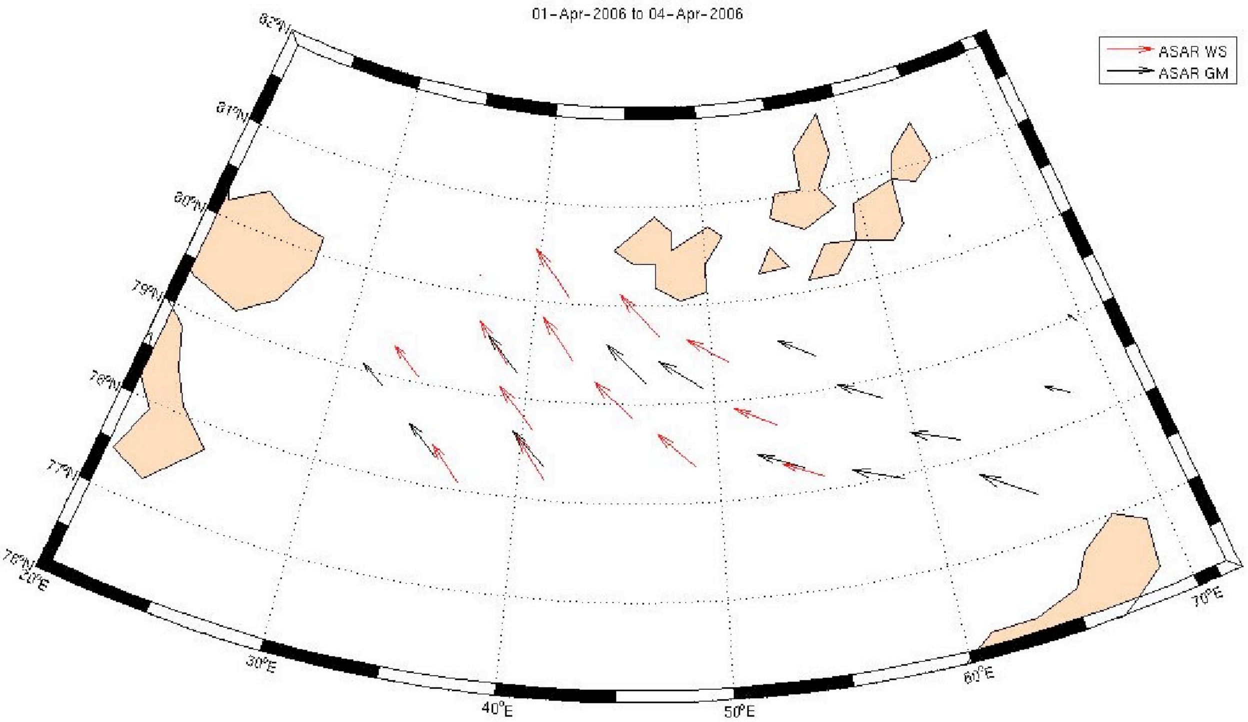

a

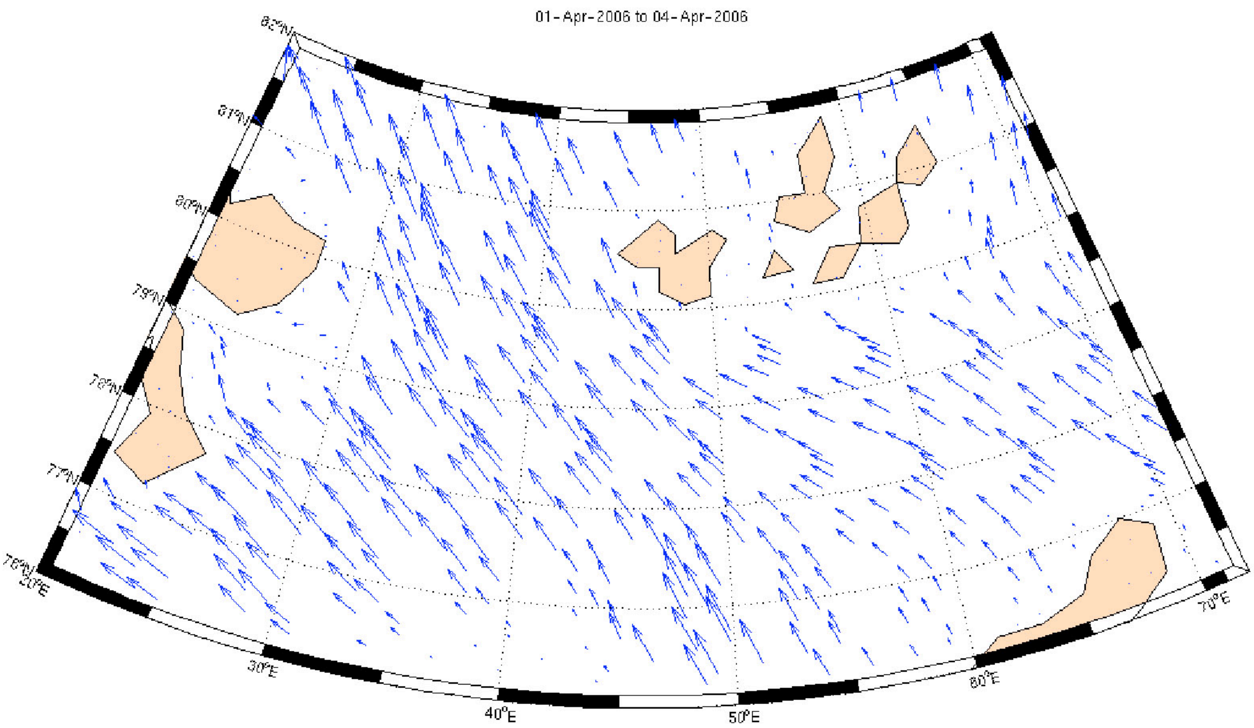

b

Figure 16. Sea ice drift from satellite data (a) and from the TOPAZ system (b) for 01 - 04 April 2006

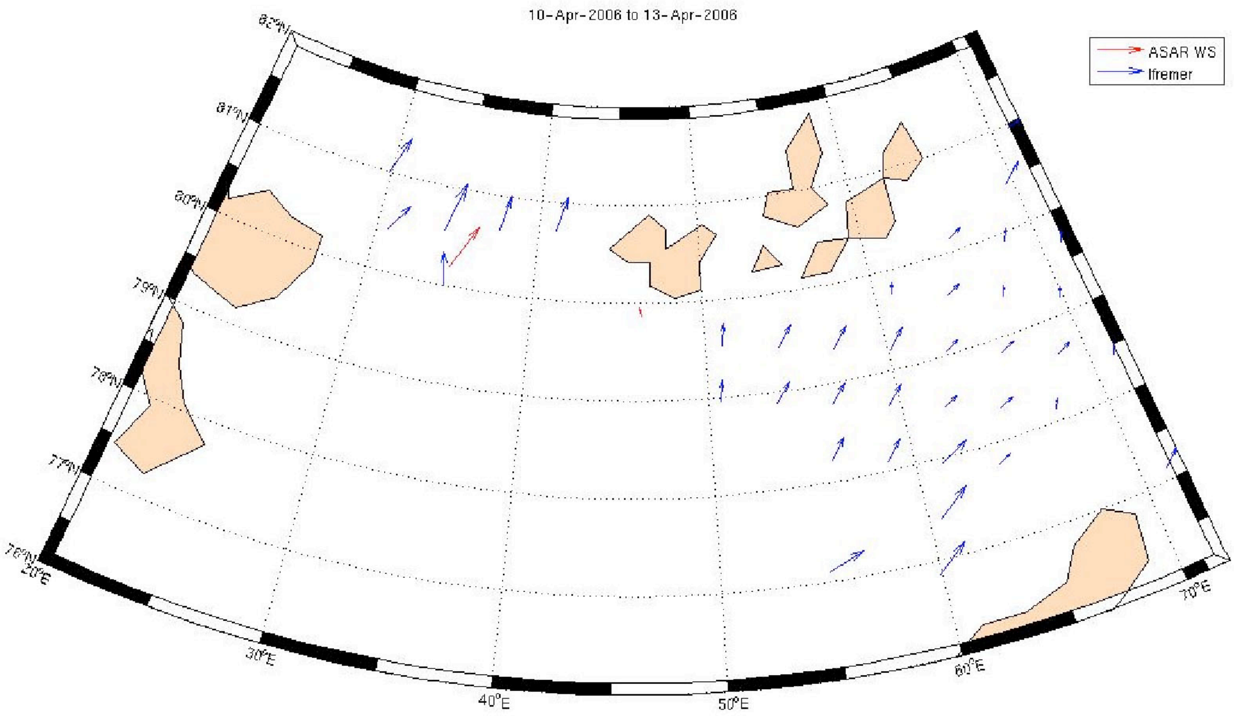

a

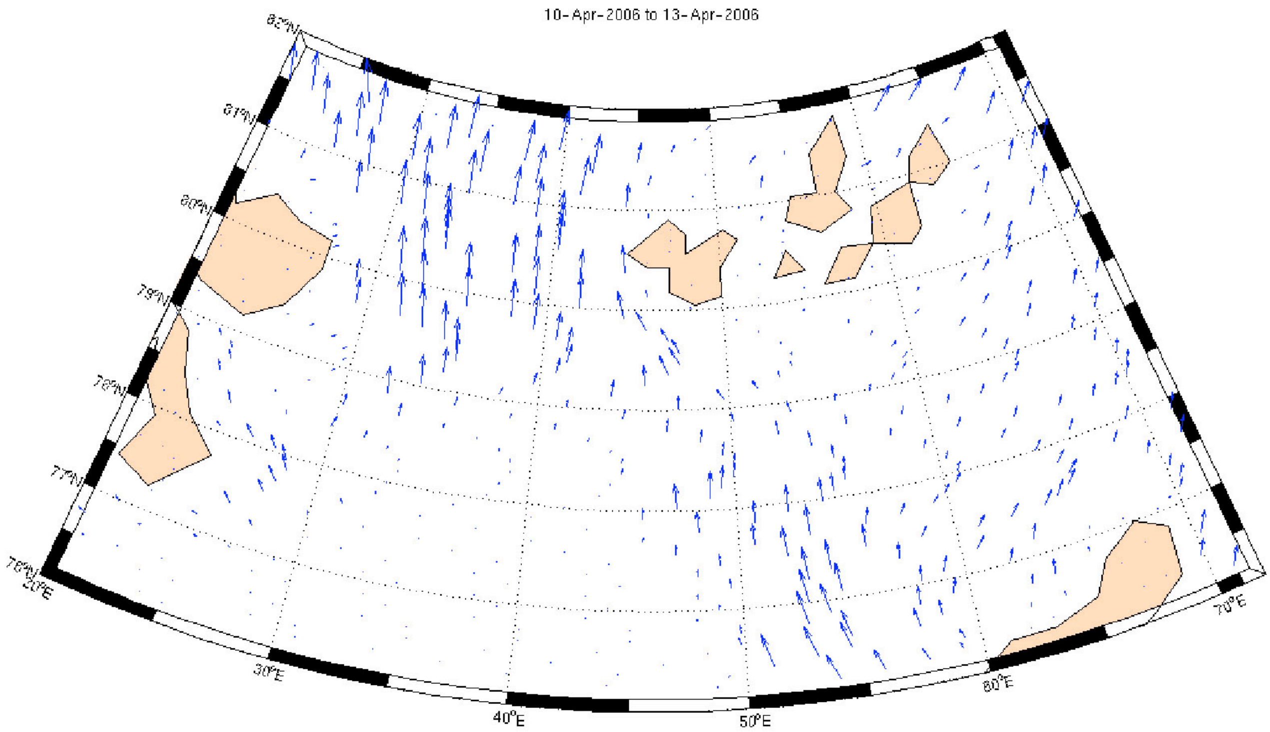

b

Figure 17. Sea ice drift from satellite data (a) and from the TOPAZ system (b) for 10-13 April 2006

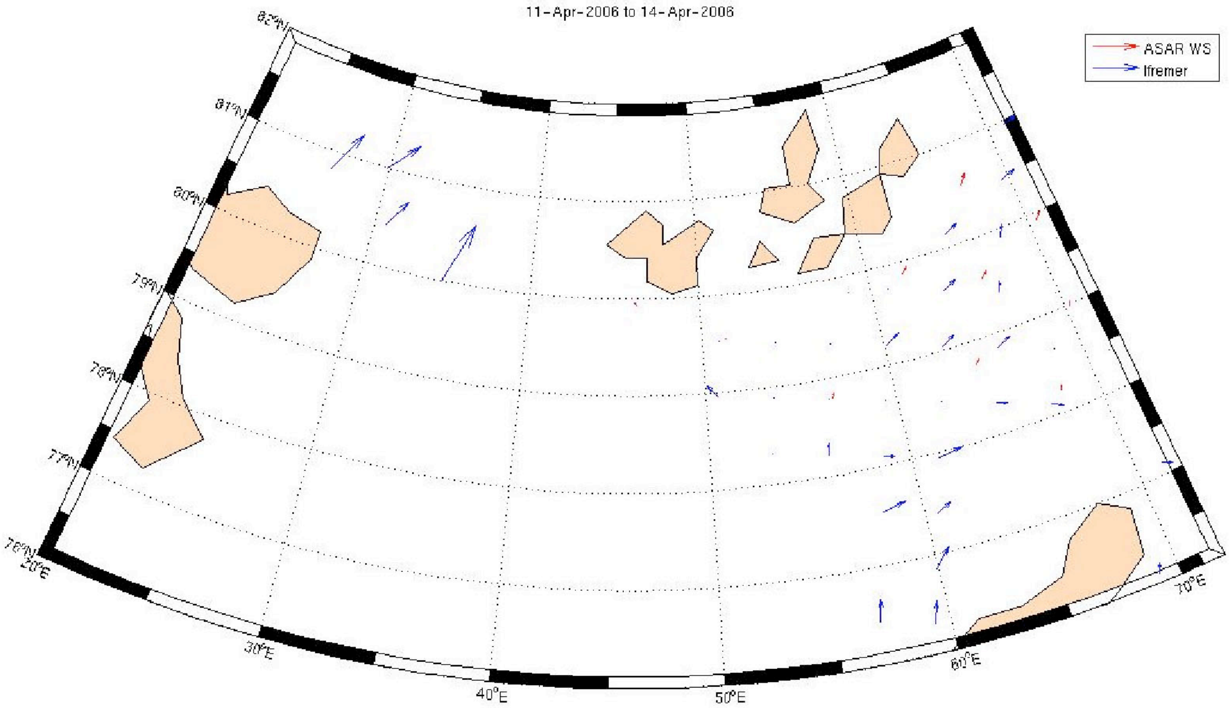

a

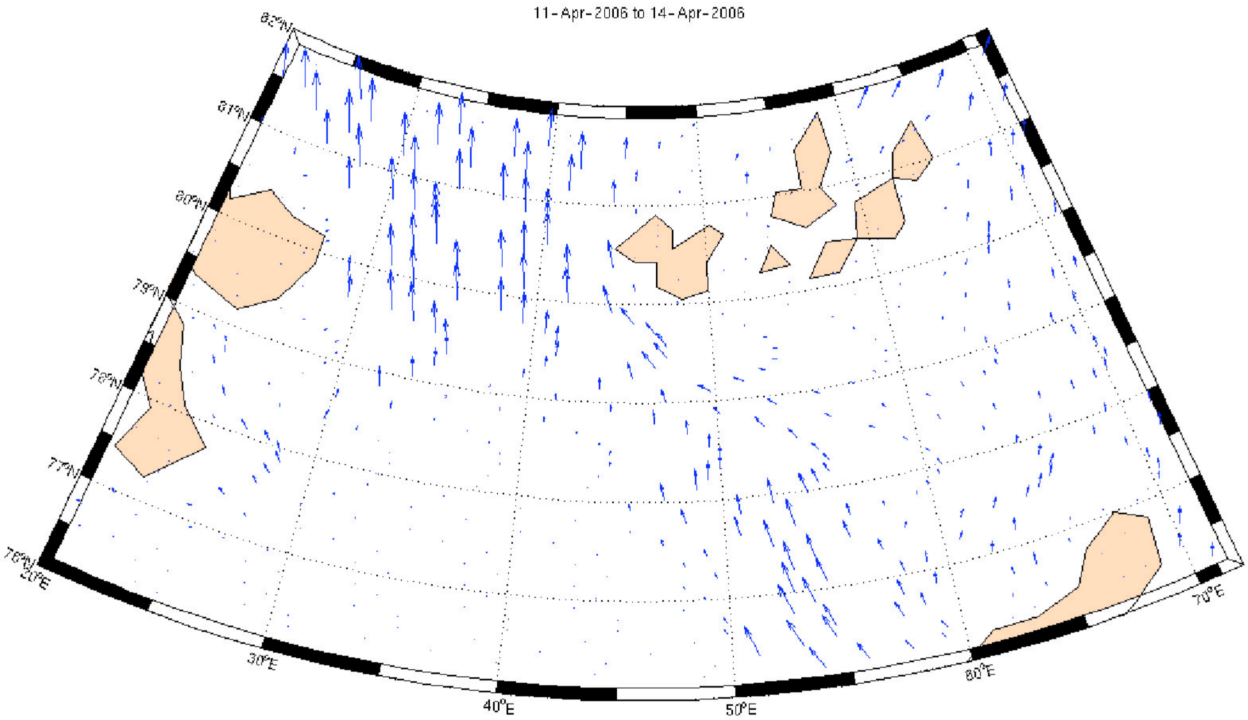

b

Figure 18. Sea ice drift from satellite data (a) and from the TOPAZ system (b) for 11 -14 April 2006

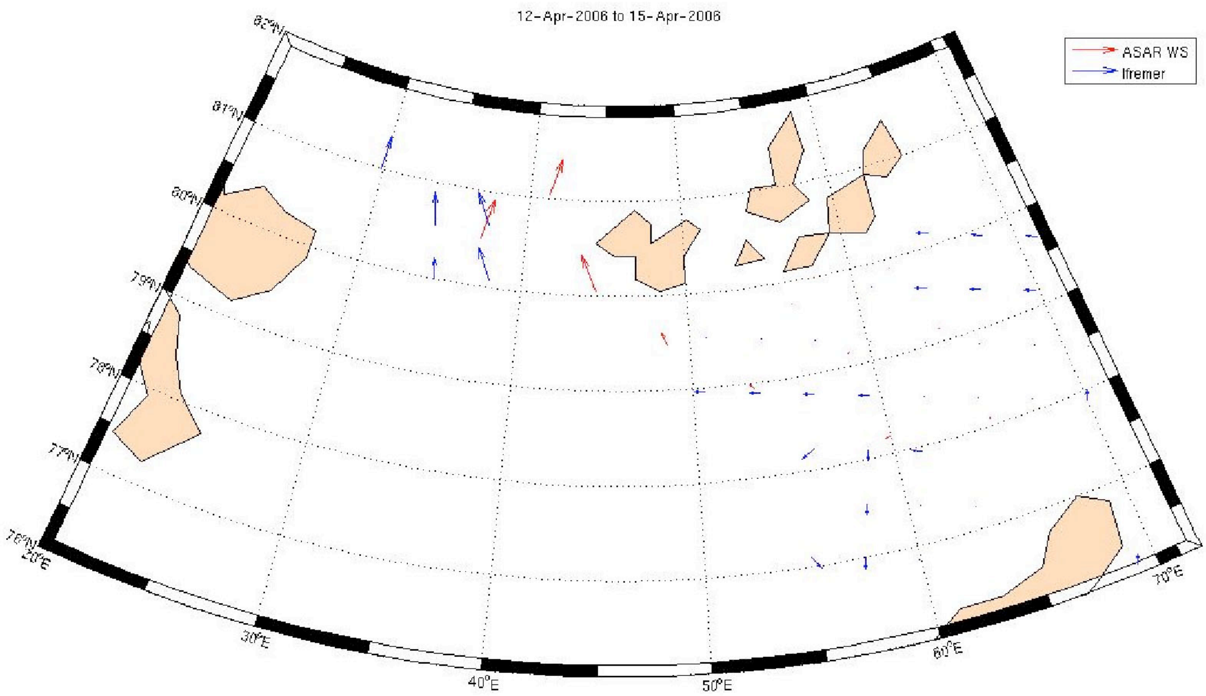

a

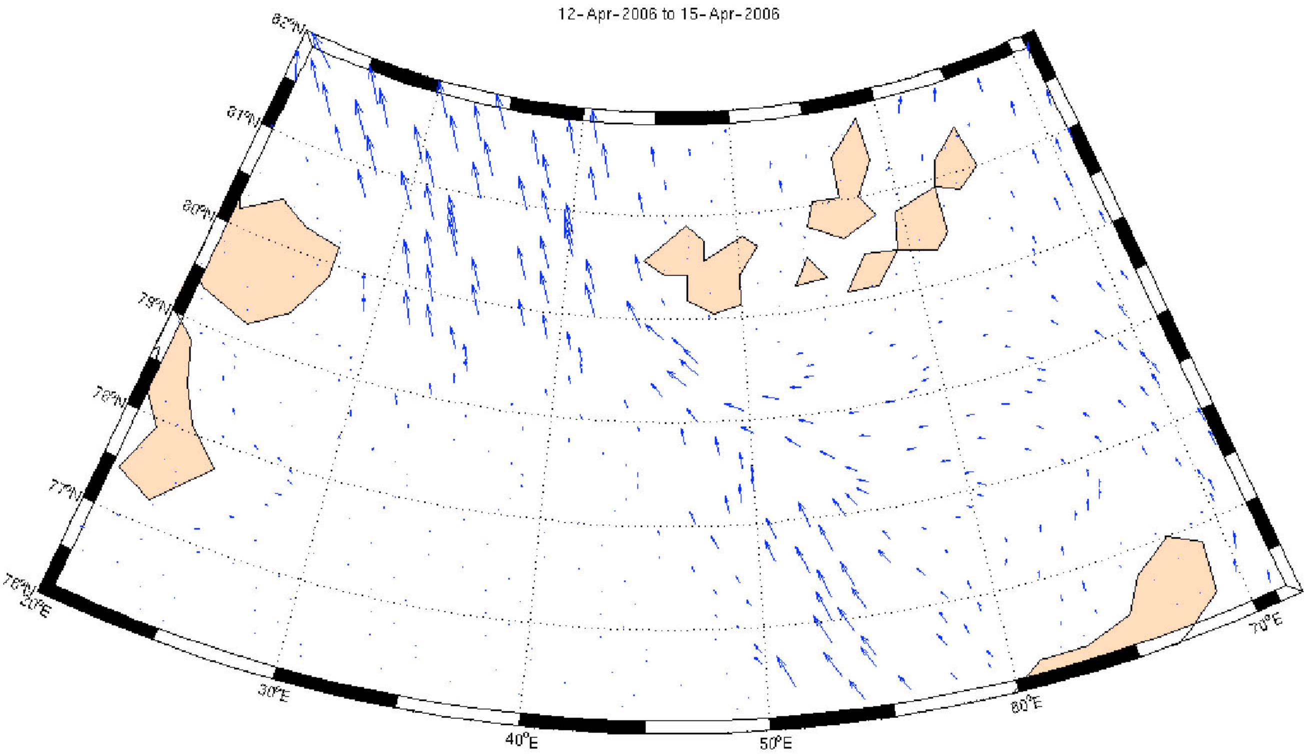

b

Figure 19. Sea ice drift from satellite data (a) and from the TOPAZ system (b) for 12 -15 April 2006

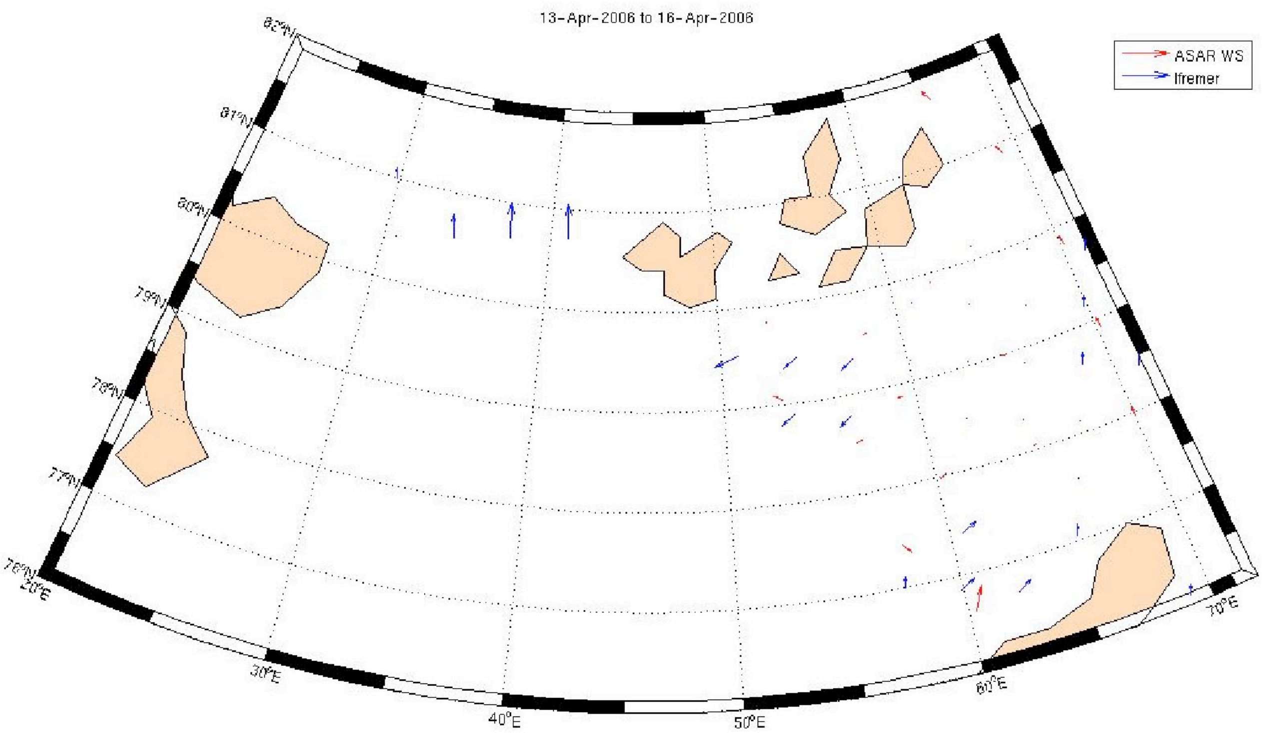

a

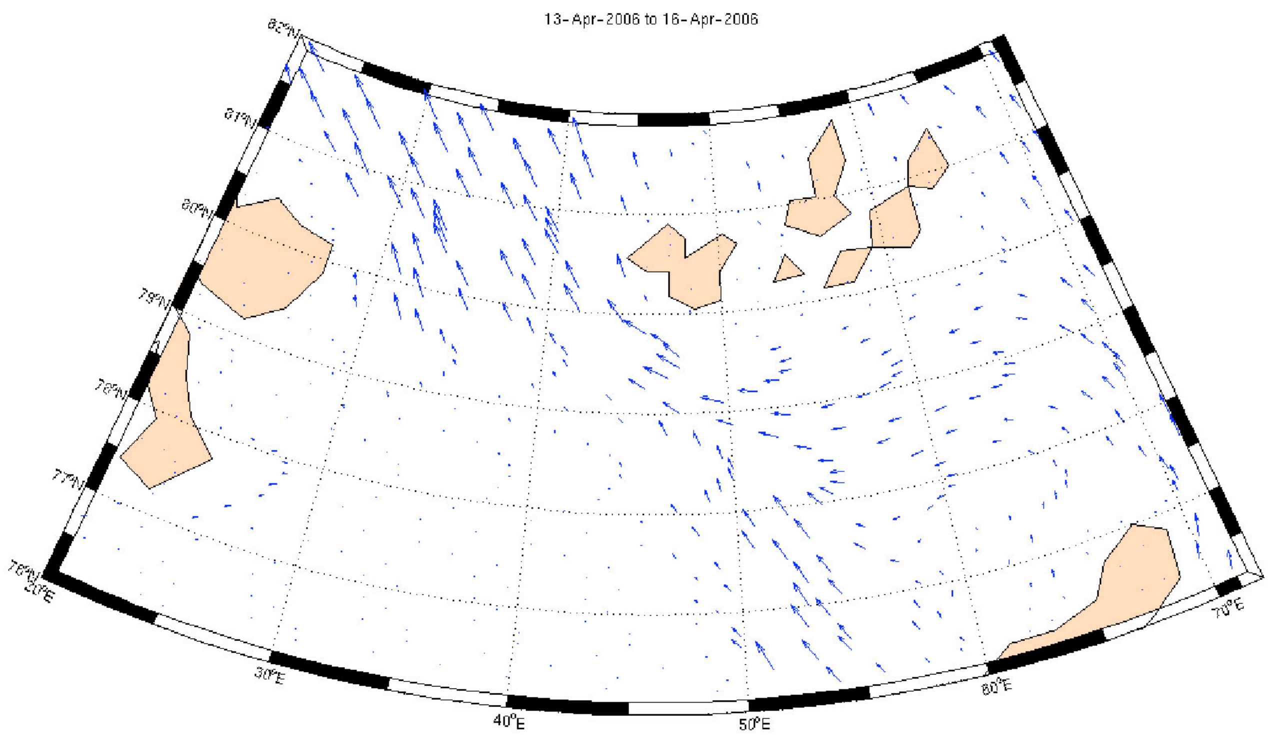

b

Figure 20. Sea ice drift from satellite data (a) and from the TOPAZ system (b) for 13 -16 April 2006

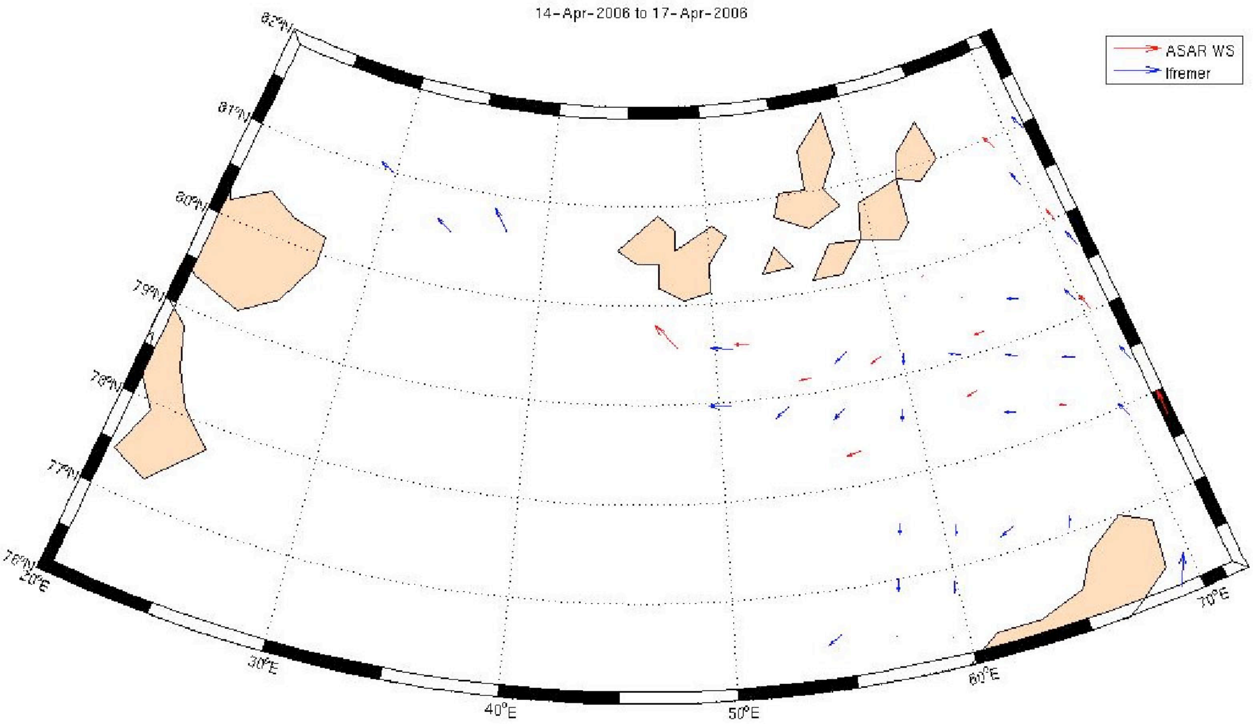

a

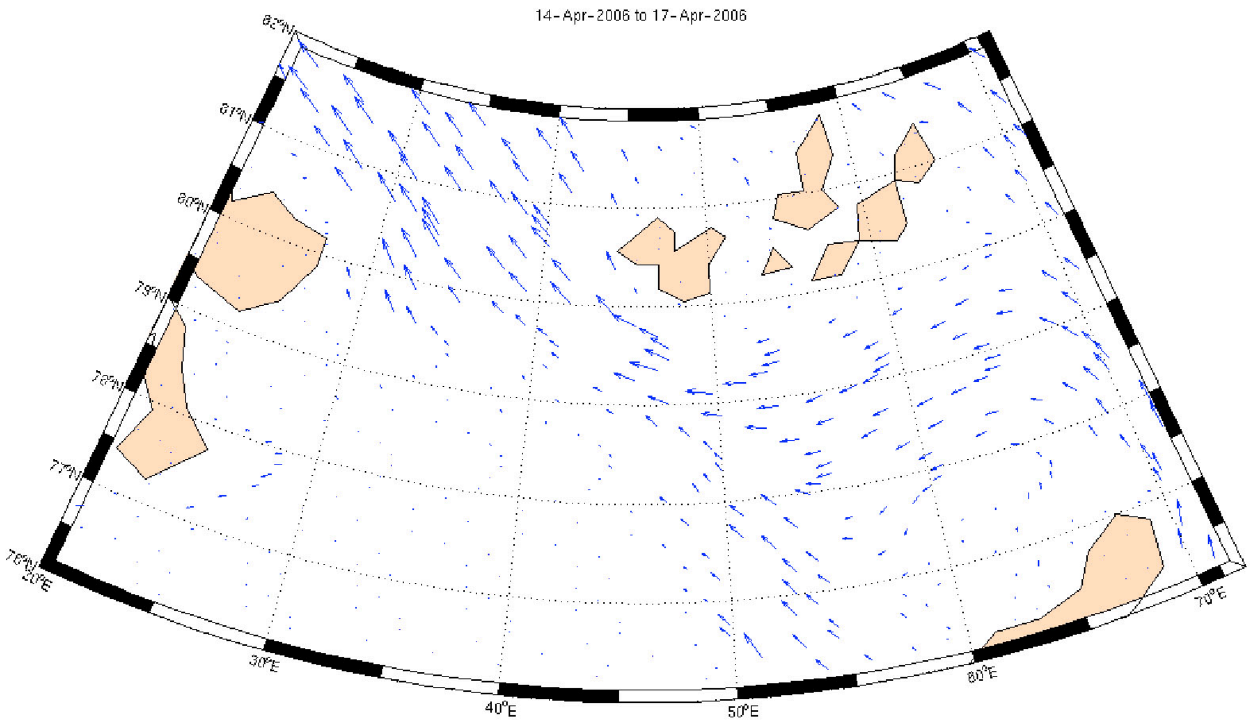

b

Figure 21. Sea ice drift from satellite data (a) and from the TOPAZ system (b) for 14 -17 April 2006

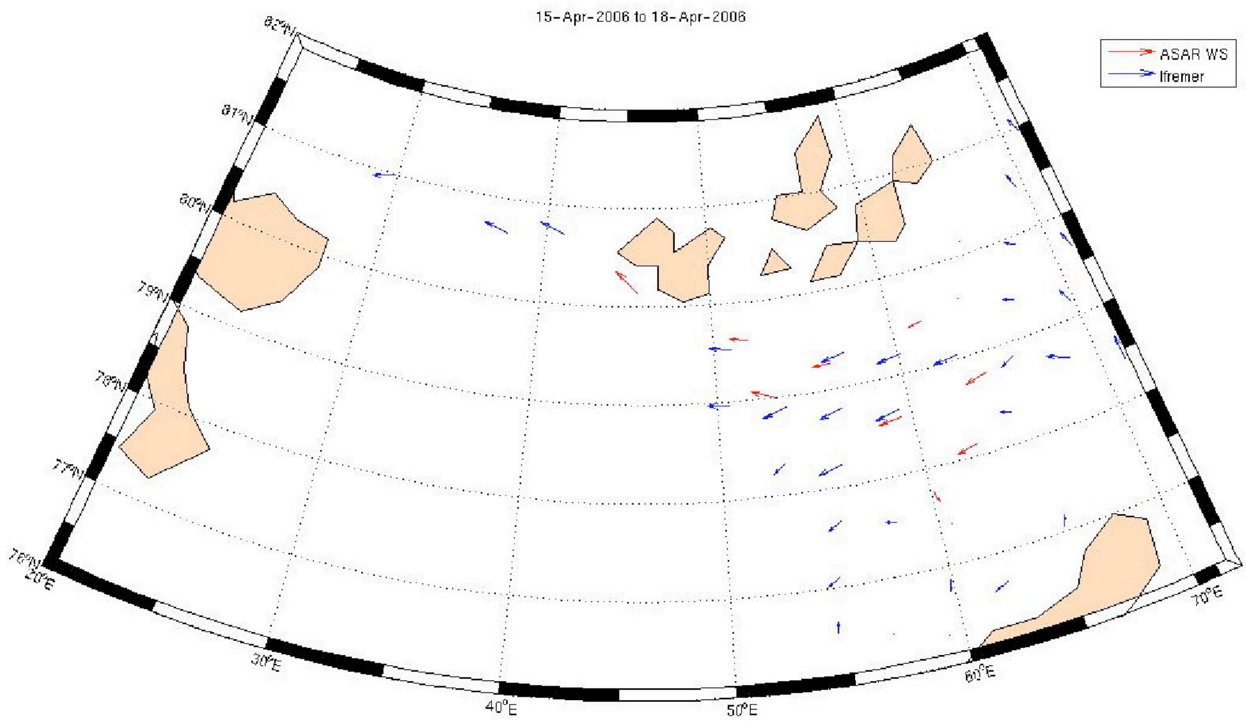

a

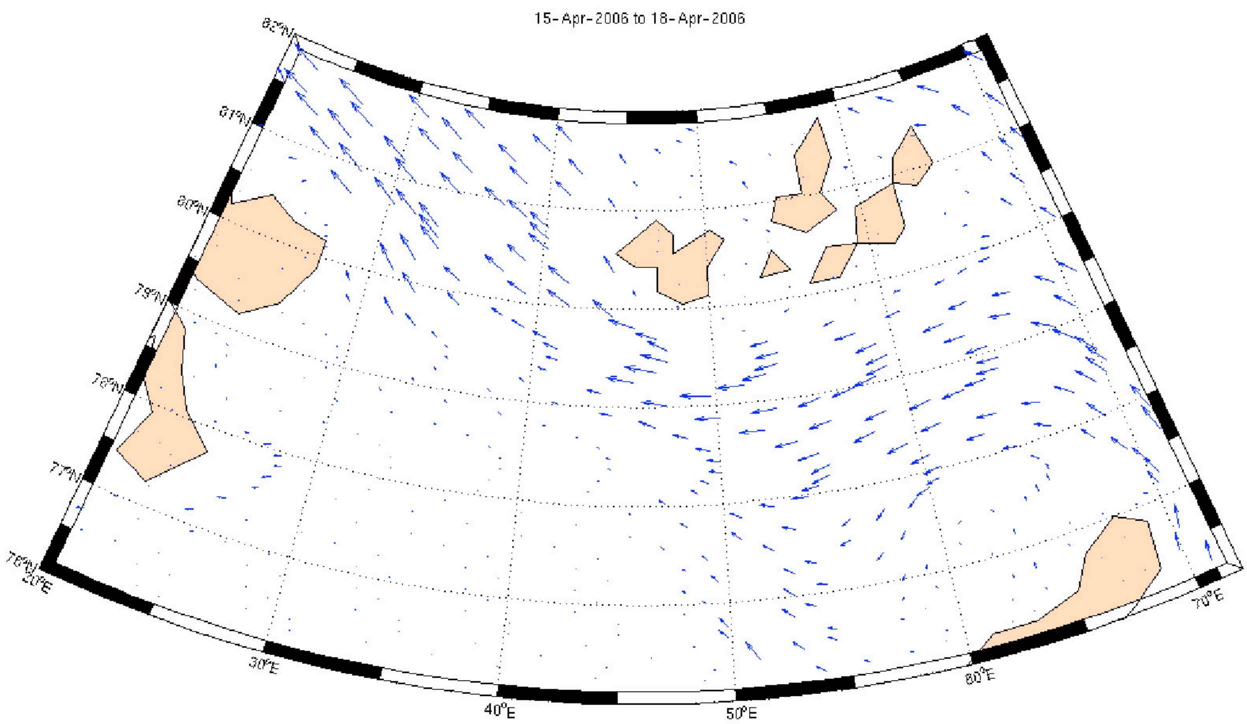

b

Figure 22. Sea ice drift from satellite data (a) and from the TOPAZ system (b) for 15 -18 April 2006

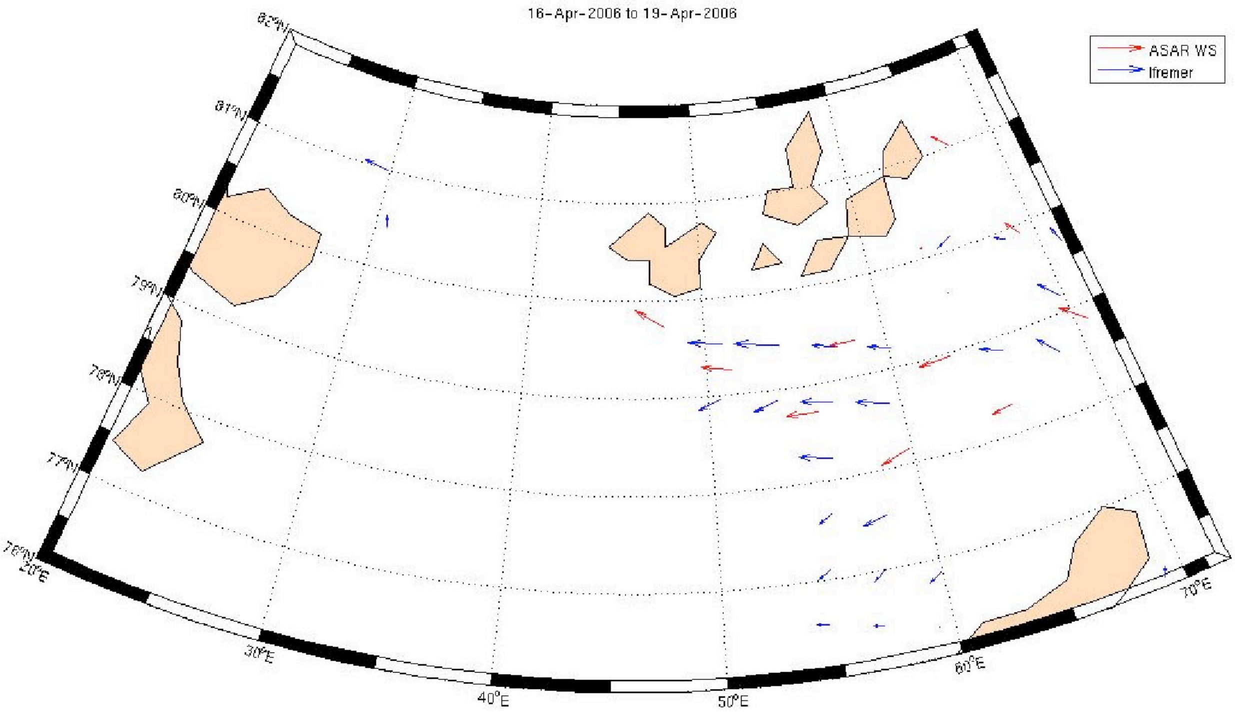

a

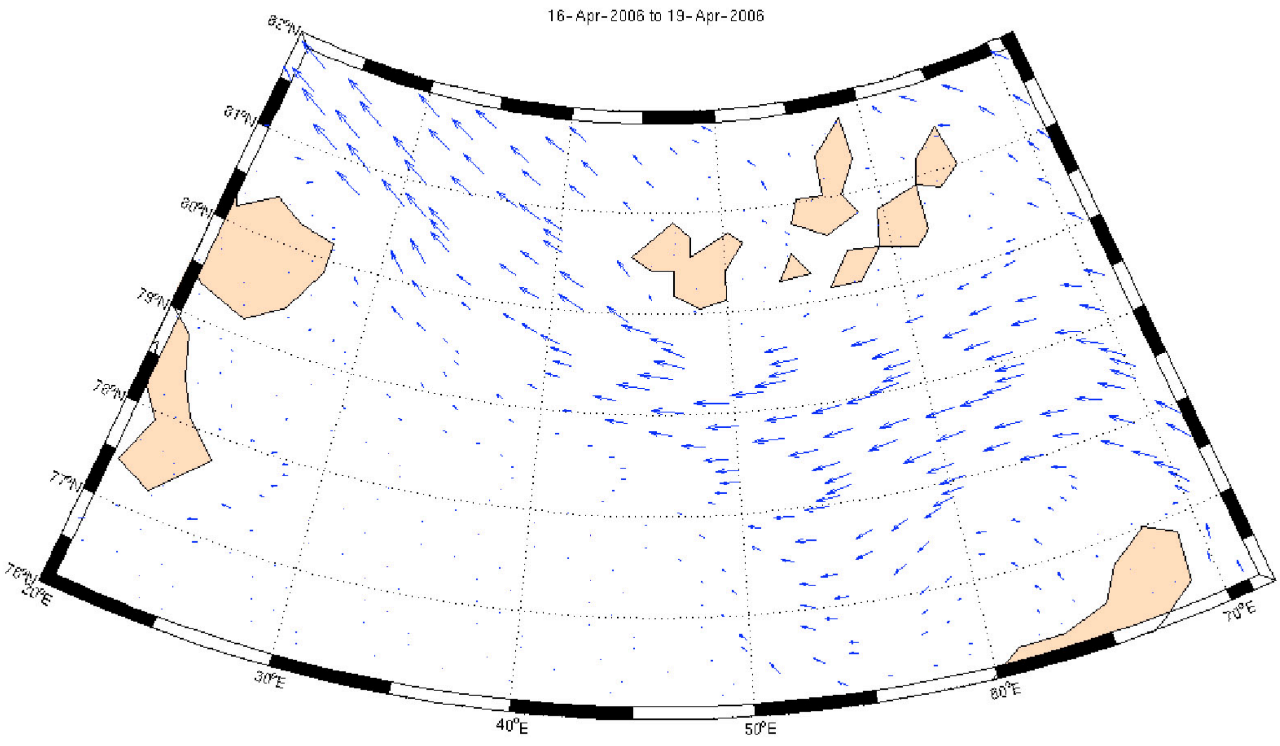

b

Figure 23. Sea ice drift from satellite data (a) and from the TOPAZ system (b) for 16 -19 April 2006

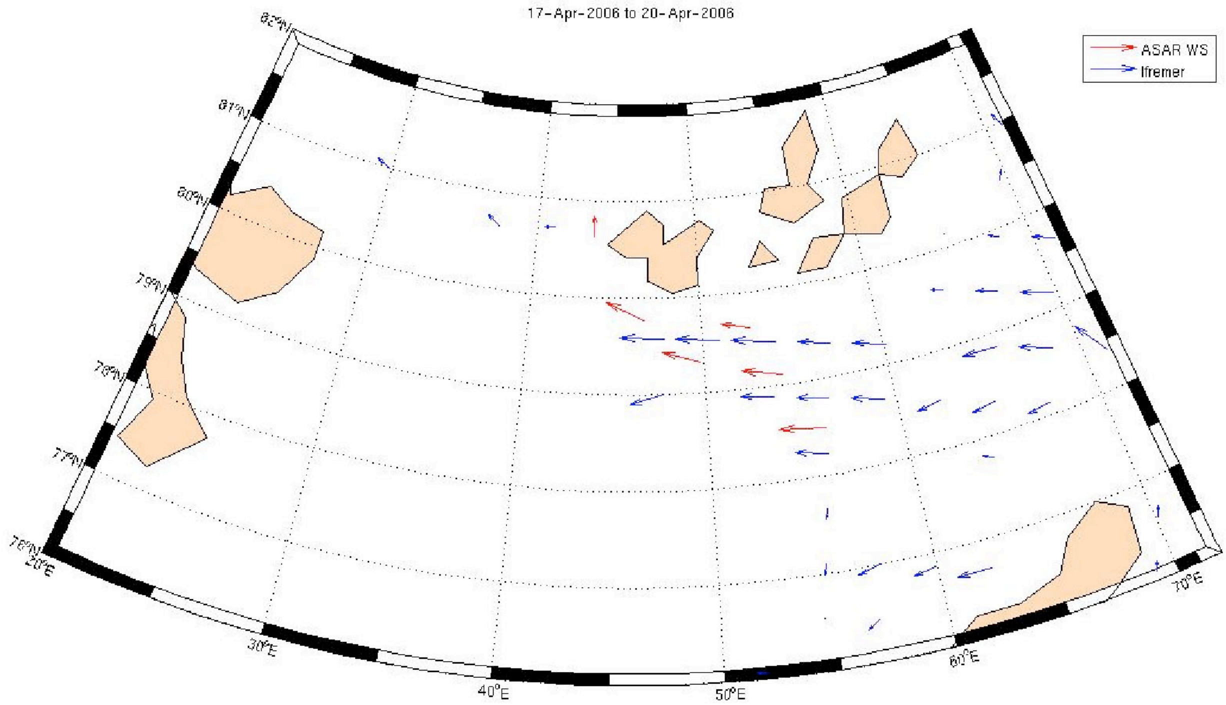

a

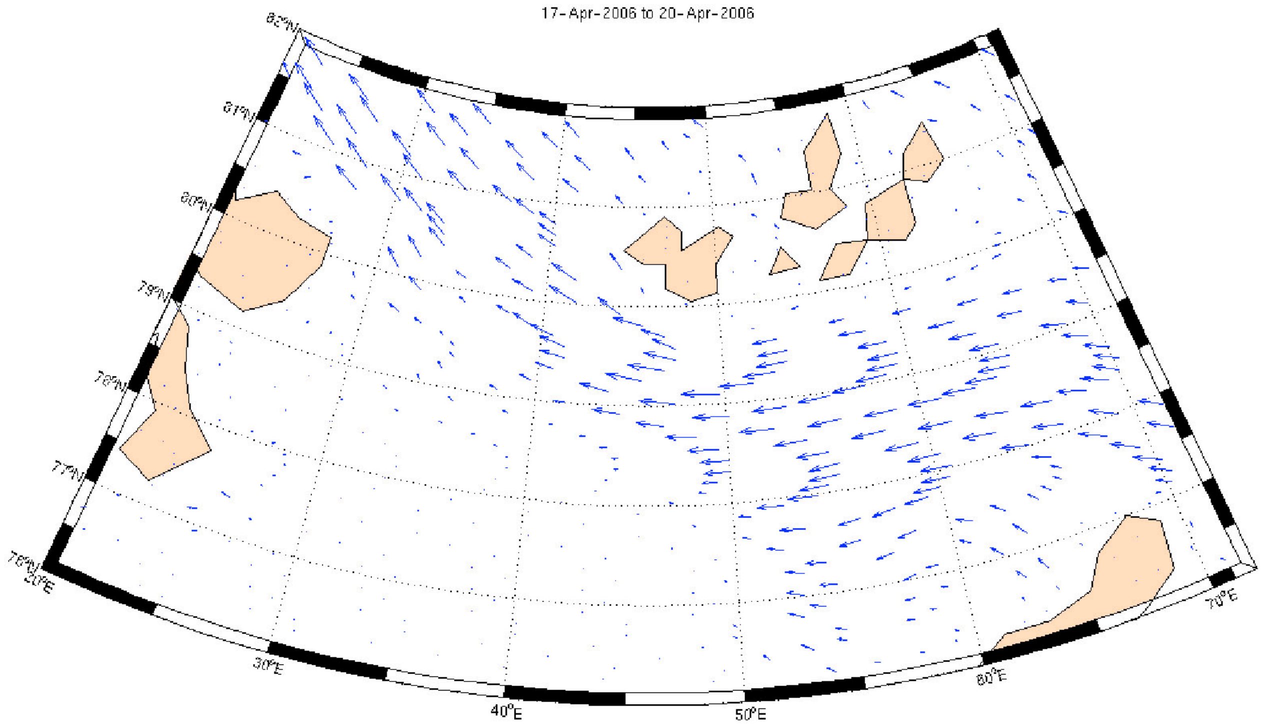

b

Figure 24. Sea ice drift from satellite data (a) and from the TOPAZ system (b) for 17 -20 April 2006

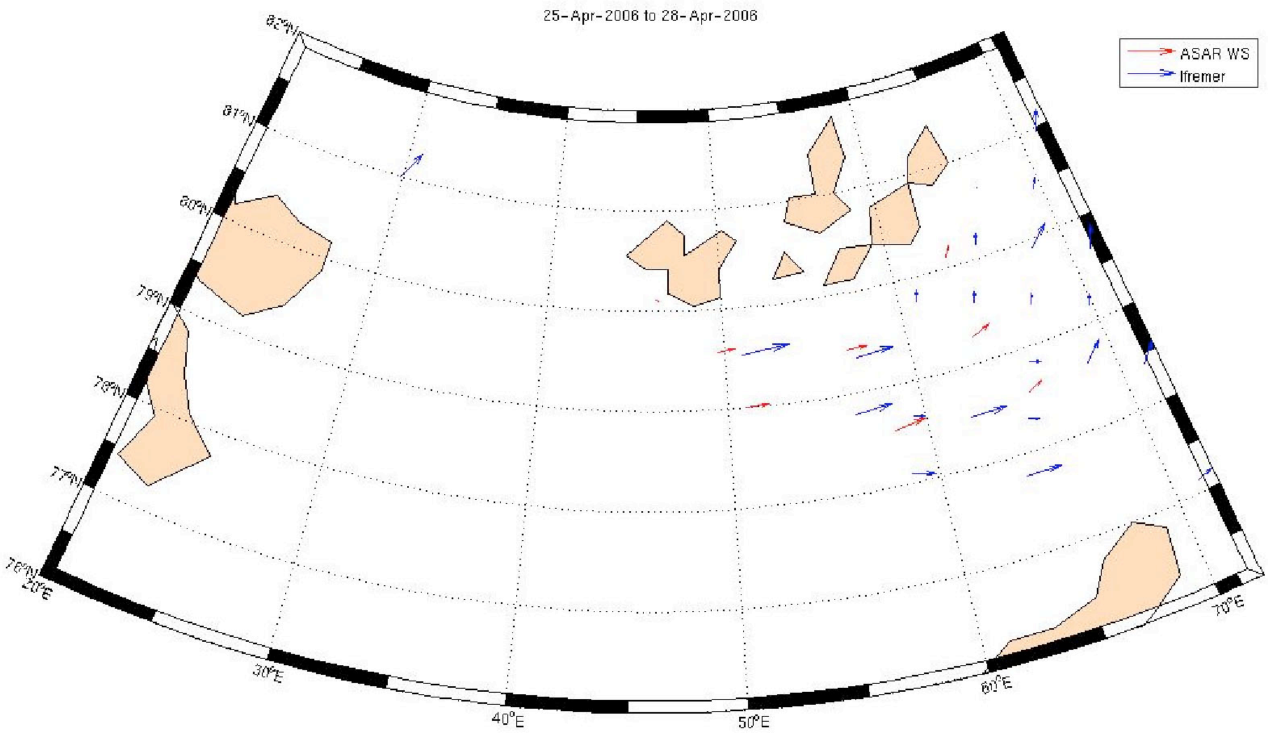

a

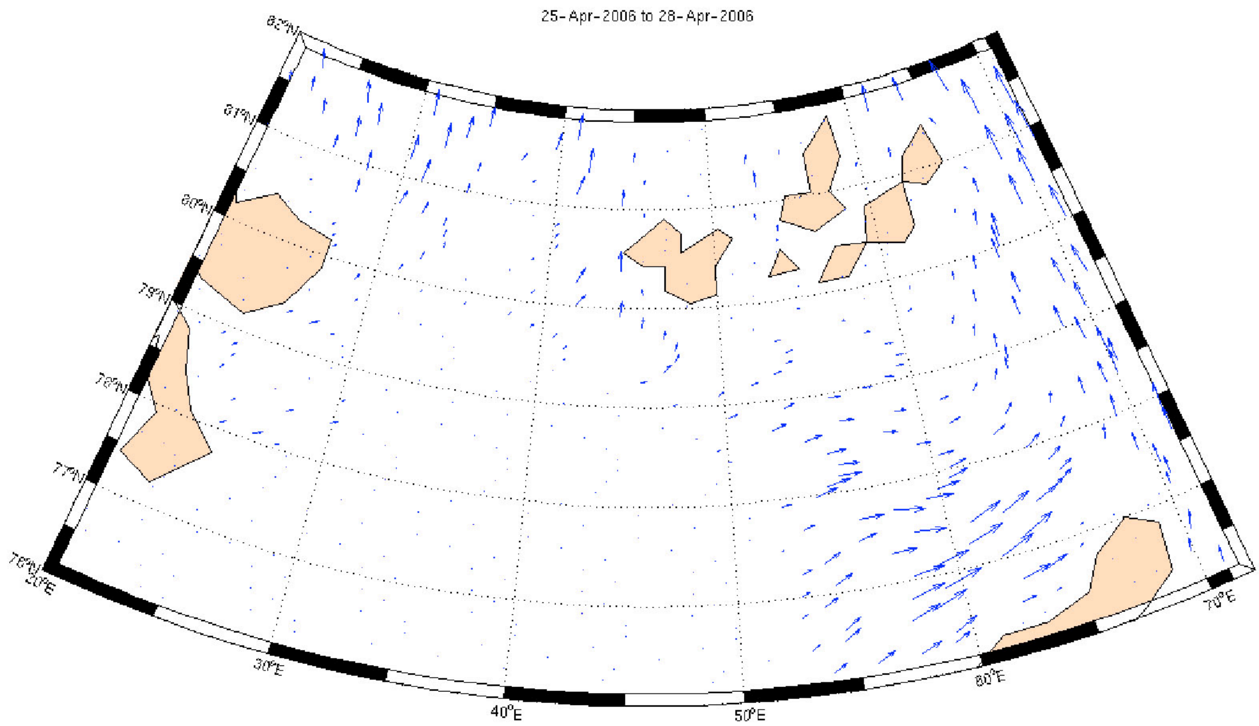

b

Figure 25. Sea ice drift from satellite data (a) and from the TOPAZ system (b) for 25 - 28 April 2006

Comparison of ice drift from Wideswath and Global Monitoring Mode SAR

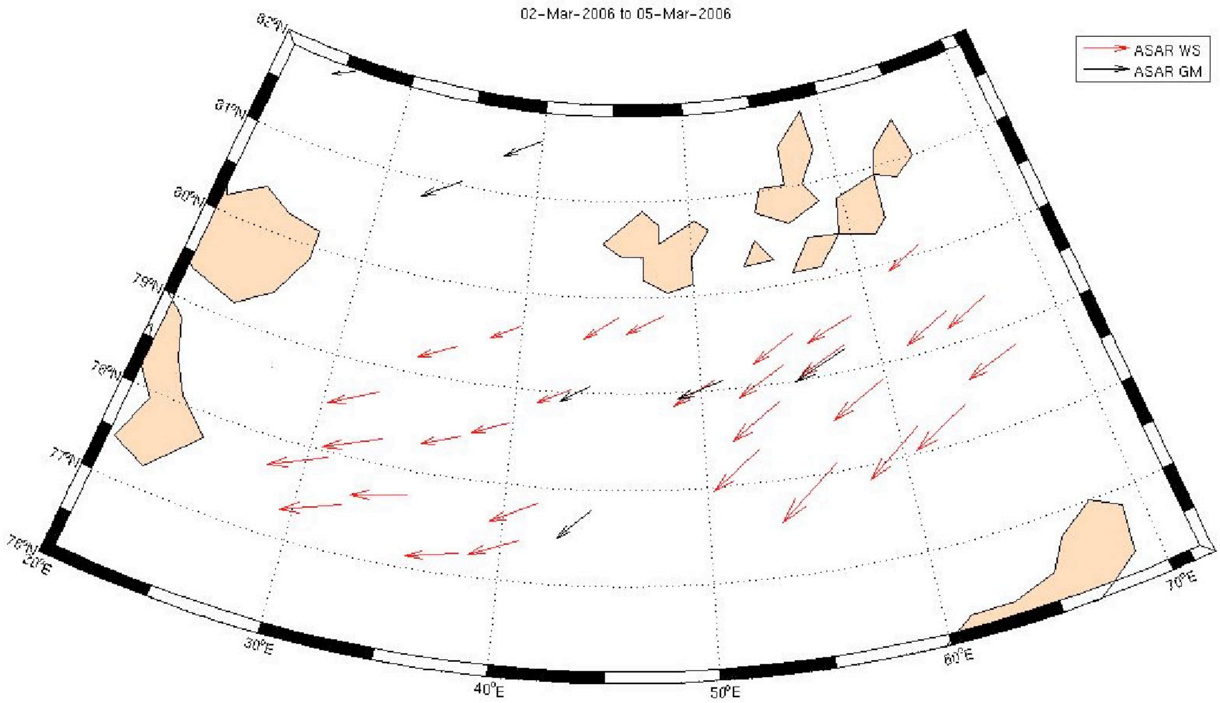

Figure 26. Sea ice drift from Wideswath (WS) and Global Monitoring ASAR for 02 – 05 March 2006

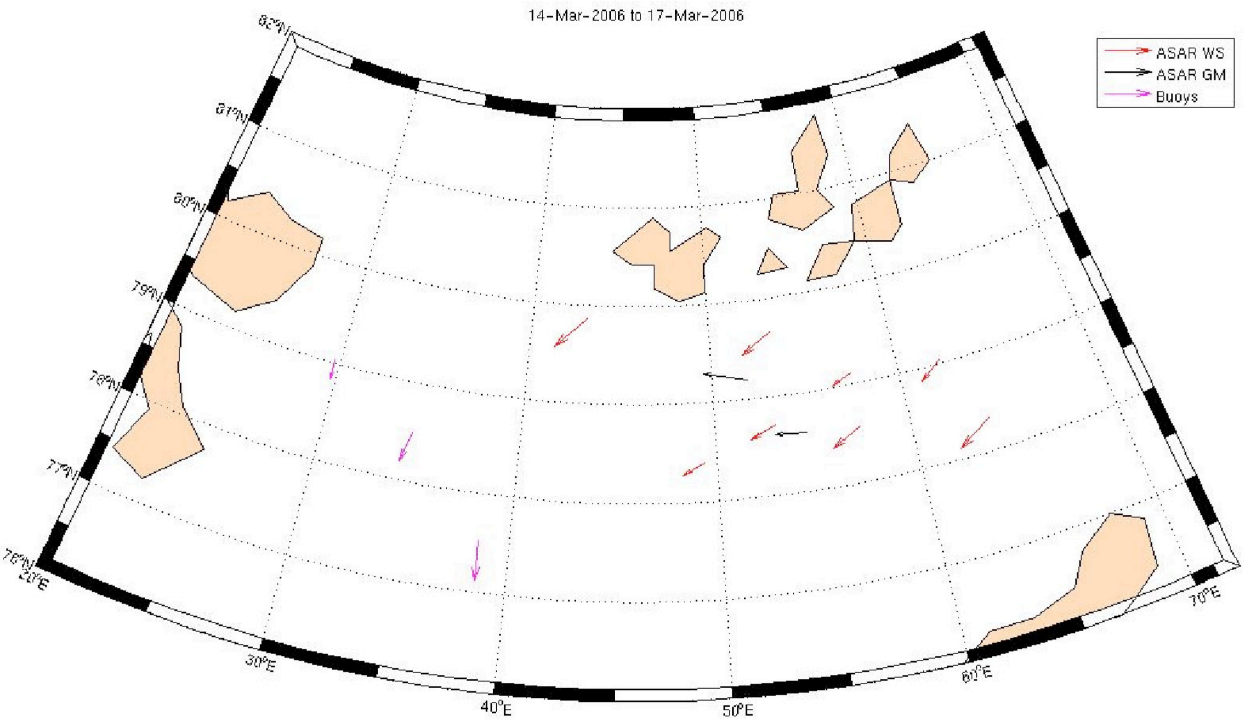

Figure 27. Sea ice drift from Wideswath (WS) and Global Monitoring ASAR including three Argos buoys for 14 – 17 March 2006

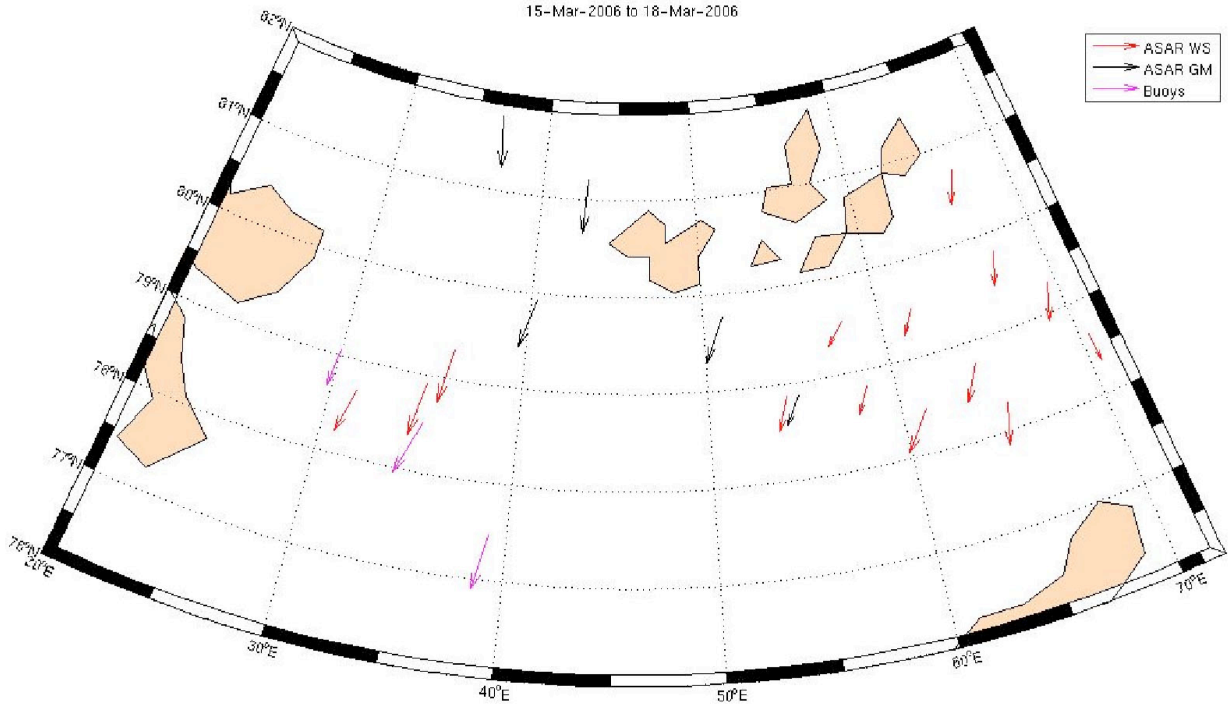

Figure 28. Sea ice drift from Wideswath (WS) and Global Monitoring ASAR including three Argos buoys for 15-18 March 2006.

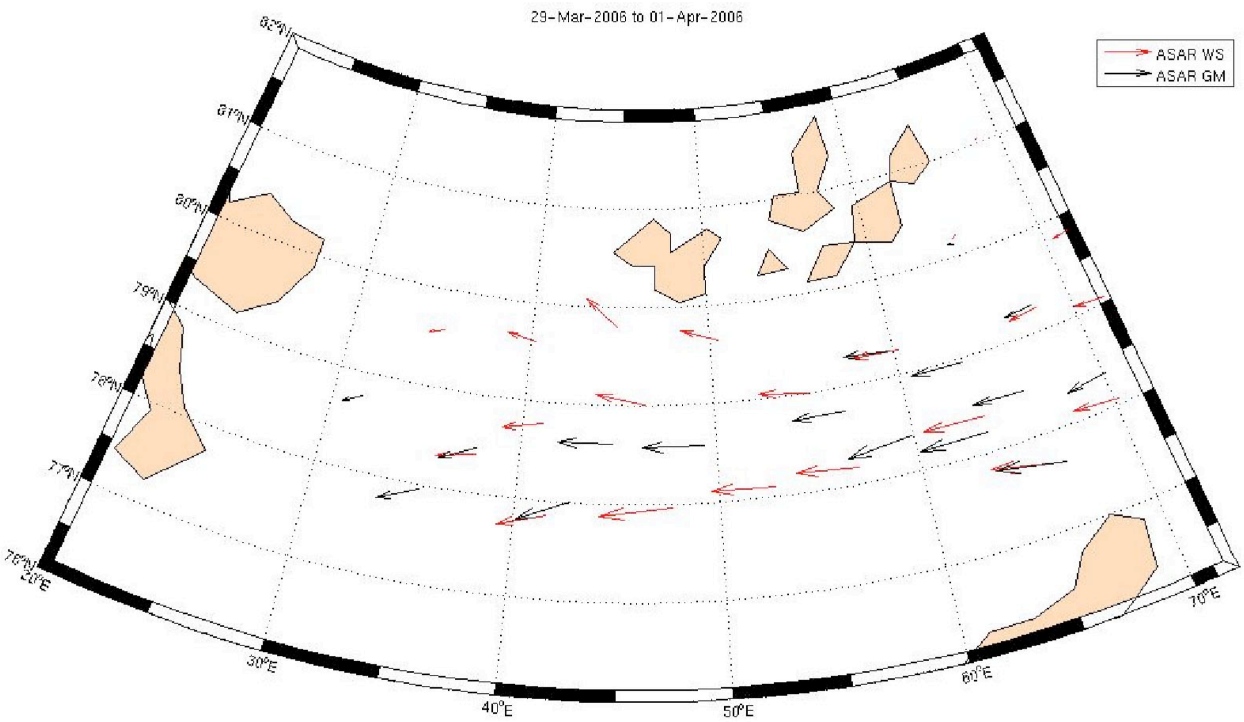

Figure 29. Sea ice drift from Wideswath (WS) and Global Monitoring ASAR for 29 March – 01 April 2006

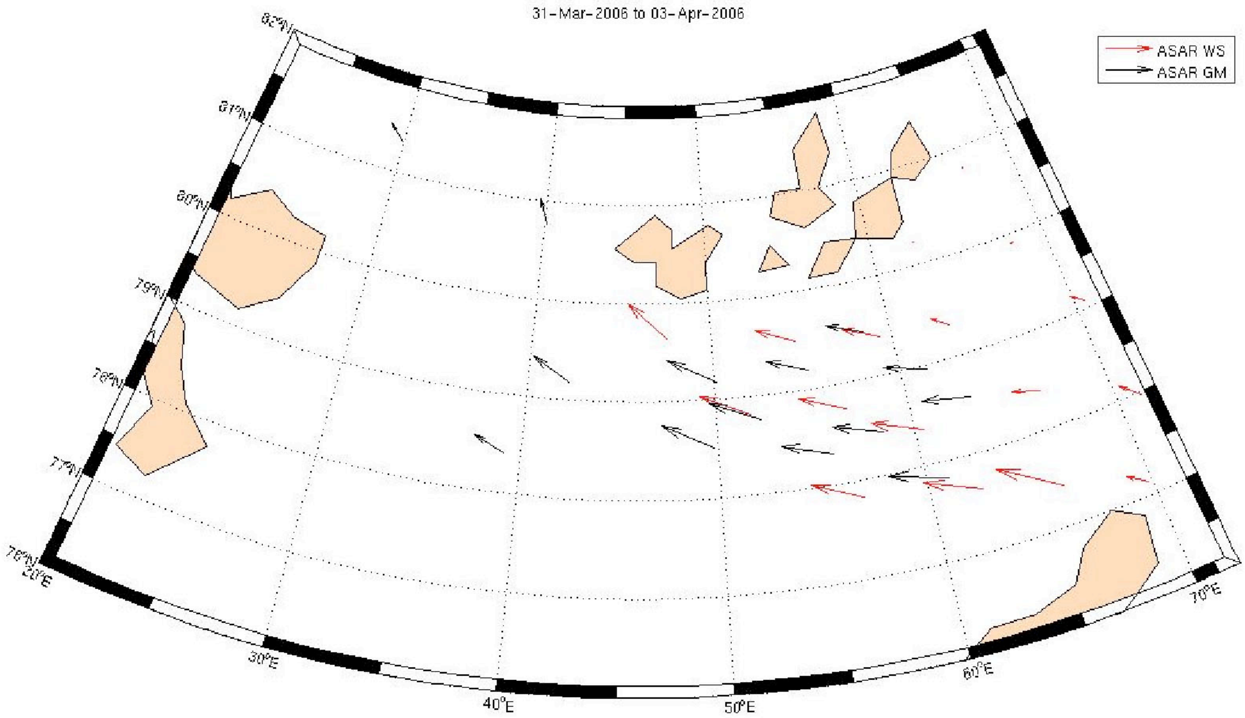

Figure 30. Sea ice drift from Wideswath (WS) and Global Monitoring ASAR for 31 March – 03 April 2006

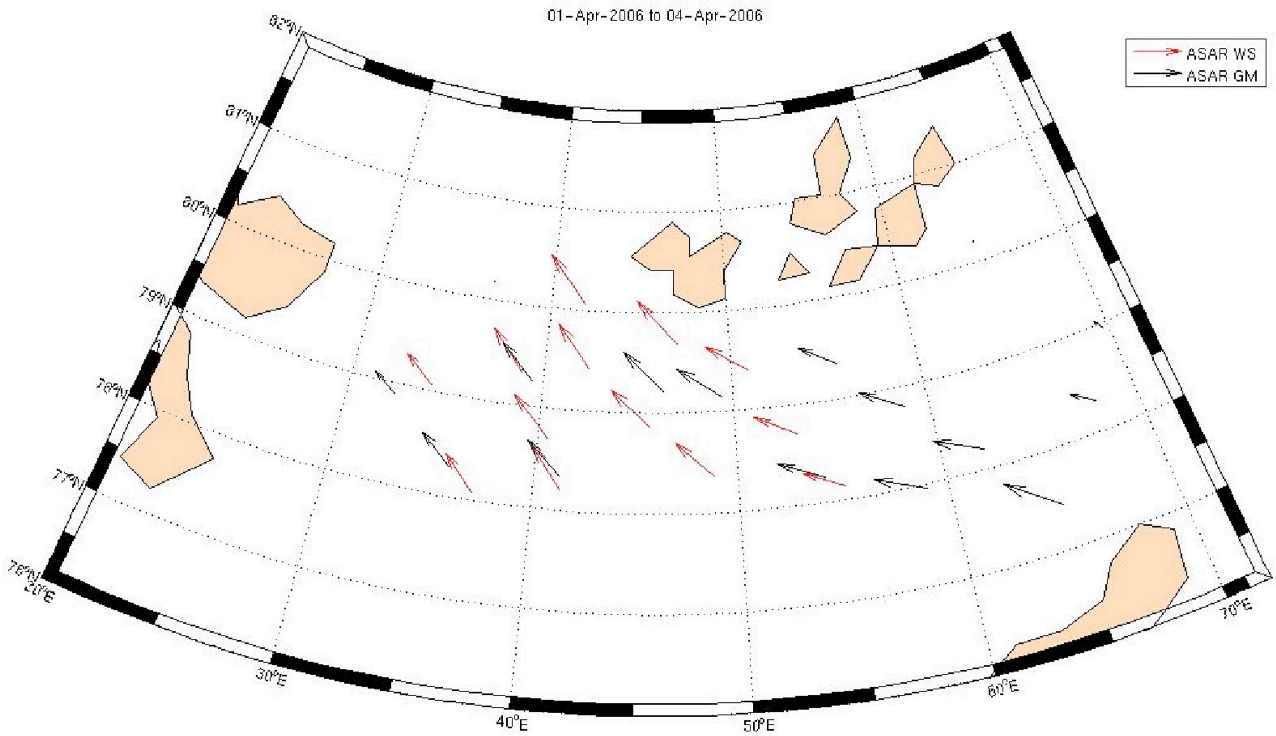

Figure 31 Sea ice drift from Wideswath (WS) and Global Monitoring ASAR for 01-04 April 2006

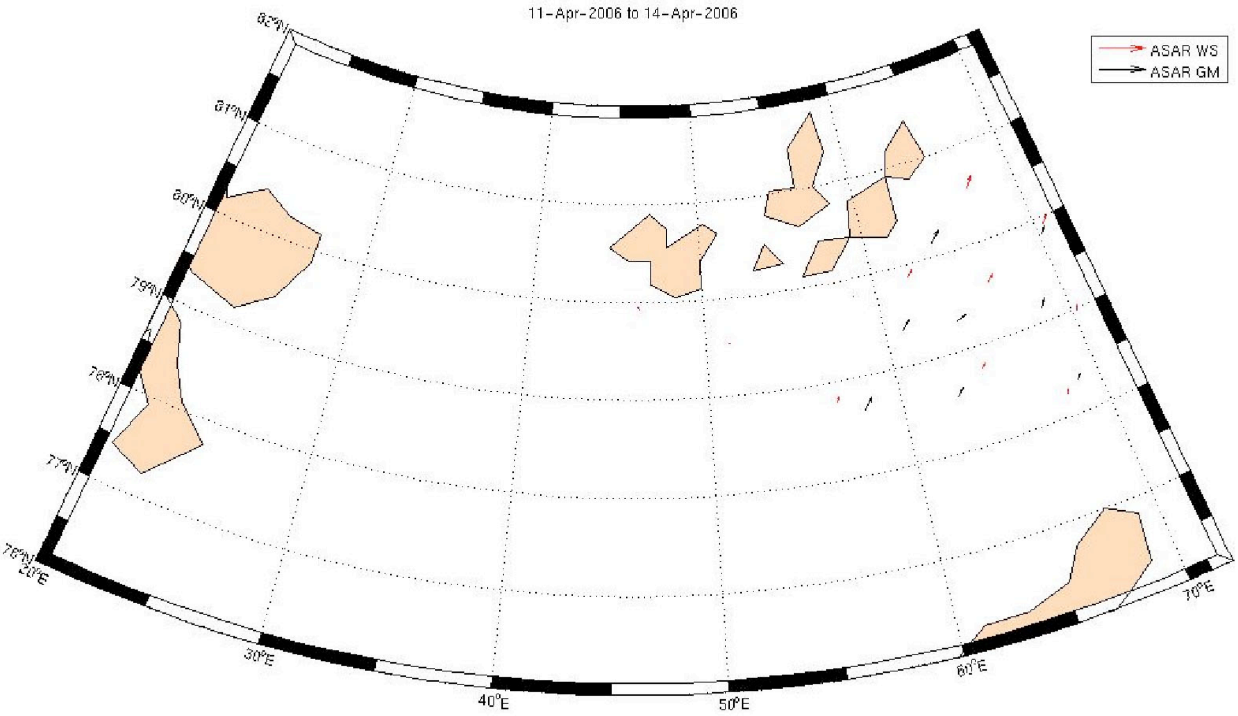

Figure 32. Sea ice drift from Wideswath (WS) and Global Monitoring ASAR for 11 – 14 April 2006

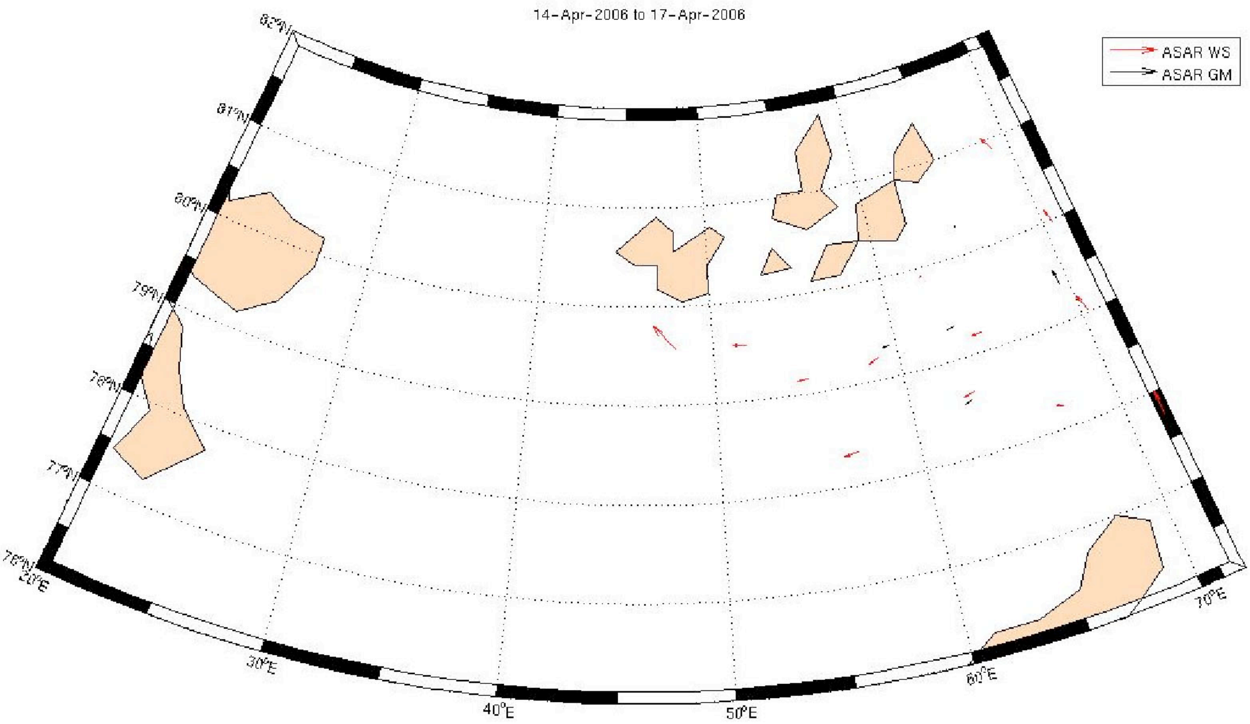

Figure 33. Sea ice drift from Wideswath (WS) and Global Monitoring ASAR for 14 – 17 April 2006

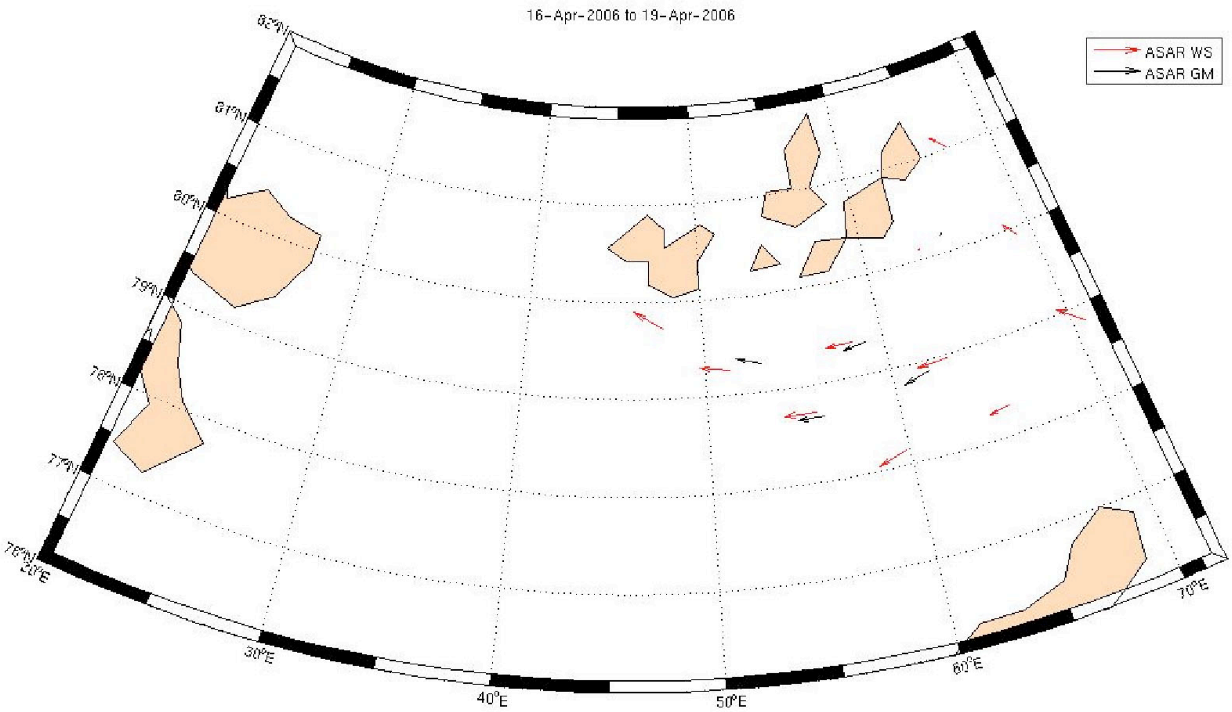

Figure 34. Sea ice drift from Wideswath (WS) and Global Monitoring ASAR for 16 – 19 April 2006

Quantitative comparison of the ice drift data

For the period 15 – 18 March, ice drift data was available from ASAR Wideswath data, Ifremer data, TOPAZ model and from three drifting Argos buoys. The ice displacement and direction for the four data sources are shown in Table 2, showing very good agreement. The data in Table 2 are taken as the mean values of each ice drift vector in the area where the drifting buoys were located in the period, as shown in Fig. 28.

Table 2. Ice displacement from satellite data, drifting buoys and TOPAZ

Period: 15-18.03	ASAR Wideswath	Ifremer data	TOPAZ model	Drifting buoys
Displacement (km)	63.0	56.9	52.2	64.4
Direction (°)	190	192	186	196

Comparison between ASAR Wideswath, Ifremer and TOPAZ data is presented for all periods in Figure 35, where ice displacement in km is shown in (a) and direction in degrees is shown in (b). There is very good agreement between the ASAR and Ifremer data, and reasonable good agreement between TOPAZ and observed ice displacement. The TOPAZ results tend to underestimate the ice displacement in km compared to observed displacement. For direction there is food agreement between TOPAZ results and the data.

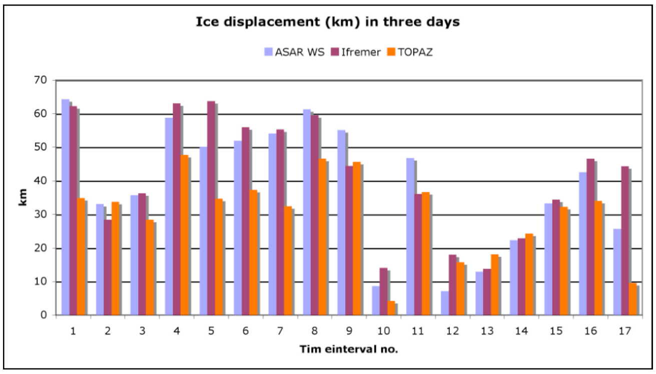

a

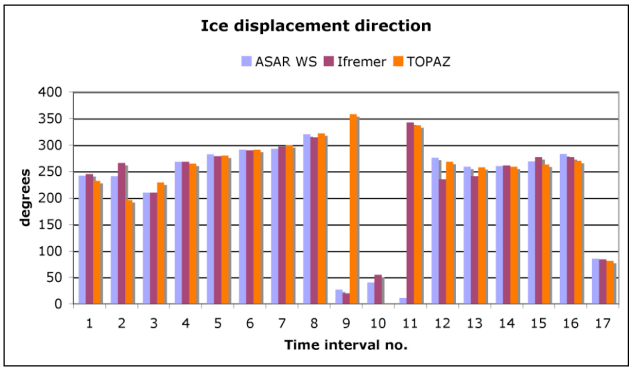

b

Figure 35. (a) Ice displacement in km for the 17 time intervals presented in table 1 for two satellite data sets (ASAR and Ifremer) and for TOPAZ model results; (b) Ice displacement direction in degrees for the same time intervals and data sources as in (a).

4. Discussion and conclusions

The winter of 2006 was characterised by extremely little sea ice in the Barents Sea. The ice edge stayed north of 76 N throughout the winter except for some scattered ice along the coast of Novaya Zemlya and in the Pechora Sea. The studies of ice drift was therefore limited to the northeastern part of the Barents Sea, including the straits beween Novaya Zemlya and Franz Josef Land, and between Franz Josef Land and Svalbard.

SAR Wideswth data collection from ENVISAT started in early March and continued until the end of May when the northeastern Barents Sea was practically ice-free. Images were collected almost every day. Overlapping images for calculation of ice drift were obtained mostly with three day interval. In addition to Wideswath data, we also collected SAR Global Mode data and estimated ice drift from these data for comparison with ice drift from Wideswath data. Comparison showed that the Wideswath data were significantly better, providing more ice drift vectors based on more accurate ice displacement estimates compared to the Global Mode data. In the 12 cases where the two data sets were compared, Wideswath data provided 141 drift vectors while Global Mode provided 60 vectors. This result is not surprising because Global Mode data has 1 km resolution compared to 100 m for Wideswath data. The latter data provides therefore much more details of the ice cover (leads, floes) needed for ice drift retrieval. The ice drift analysis was performed by manual analysis to ensure that the ice drift vectors are as accurate as possible.

The ice drift vectors from SAR were plotted on maps together with ice drift vectors provided by Ifremer. These are based on scatterometer and passive microwave satellite data and are produced for the whole Arctic sea ice area. The Ifremer vectors show very good agrement with the SAR Wideswath data, although the Ifremer data are based on coarse resolution satellite data. In other areas of the Marginal Ice Zone, such as the Fram Strait, studies have shown that the Ifremer ice drift was less accurate compared with SAR derived ice drift. Neither Ifremer nor SAR ice drift products provided estimates in the ice edge region near open water. The reason for this is that it is difficult to find ice features that are stable enough to last for several days and can be recognised i a series of images. The satellite-based ice drift vectors cannot be produced with regular spatial coverage in this region because images did not cover the same area at every time interval (the SAR data) and the Ifremer products did not provide full coverage of ice drift data, leaving many grid cells without data. Nevertheless, the satellite-based ice drift provided enough data to get an overvall picture of the ice drift in the region, including the fluxes through the straits. The satellite data also provided a good data set for validation of the modelled ice drift from the TOPAZ forecasting system.

Ice drift data were also obtained from three buoys deployed on ice floes east of Svalbard. These buoys were deployed in early March by CMR under contract with Statoil. The buoys drifted southwestwards reaching open water in early April, providing about one month of ice drift data. The comparison between the buoys data and the satellite-retrieved data was done for the period 15 – 18 March, showing good agreement between the two data sets.

Comparison of ice drift data with modelled ice drift from the TOPAZ system is important for validation of the foreceasting capability of the sea ice model in TOPAZ. The iceberg model which is part of the high-resolution Barents Sea model under development at NERSC, is nested with the TOPAZ system at the model boundaries. For the Barents Sea model it is necessary to have good validation of ice drift and other model parameters at the boundaries. The data set presented in this report is the first validation data for ice drift, showing an overall good quality of the modelled ice drift.

In the priod from early to mid March, the ice drift was generally directed in a southwesterly direction with inflow of ice to the Barents Sea through the straits between Novaya Zemlya and Franz Josef Land and between Franz Josef Land and Svalbard. From 28 March to 04 April, the ice drift was more westerly, turning northwesterly with ice drift out of the Barents Sea between Franz Josef Land and Svalbard. From 10 to 20 April the drift varied between northerly and northeasterly, with occasional eastward drift through the strait between Novaya Zemlya and Franz Josef Land. This agrees well with the ice charts showing that the ice edge was pushed significantly to the north during April. The maximum ice drift, averaged over three days, was found to be about 0.30 ms^{-1} in early and mid March for southwesterly drift.

In conclusion, the first study of ice drift with SAR data in the northeastern Barents Sea was performed in March- April, showing good agreement with other ice drift data provided from scatterometer and passive microwave data as well as with buoy drift data. The ice drift data were used to carry out a first validation of ice drift produced by the TOPAZ system. The visual comparison between obsvered and modelled ice drift showed good agreement, but further and more quantitative validation is needed. Satellite data can provide a reasonably good synoptic picture of the ice drift over large areas, in contrast to drifting buoys which can only provide data in a few locations, depending on how many buoys are in operation. Buoy data, however, provide continuous and very accurate measurements of the ice drift. The present study has used three day interval for the ice drift, but it is necessary to compare ice daily averaged ice drift, because we know that ice drift can change rapidly in this region due to changing wind forcing. It is important to assess how well satellite data can be used for monitoring daily ice drift.

Data on sea ice drift will be an important component of the validation of the Barents Sea model which includes an iceberg drift model. Data on iceberg drift can only be obtained by deploying ARGOS/GPS drifters on selected icebergs. The iceberg drift is a function of the sea ice properties such as concentration, thickness and speed. It is recommended to continue observation of sea ice properties as part of the iceberg modelling work in the Barents Sea. The goal for this work is to come up with a monitoring and forecasting system for sea ice and icebergs, using numerical models in combination with satellite data and drifting ice buoys.